The Geological Society of America
Special Paper 544

Cretaceous-Paleocene transition along a rocky carbonate shore: Implications for the Cretaceous-Paleocene boundary event in shallow platform environments and correlation to the deep sea

Diethard Sanders*
Institute of Geology, Faculty of Geo- and Atmospheric Sciences, University of Innsbruck, A-6020 Innsbruck, Austria

Gerta Keller
Department of Geosciences, Princeton University, Princeton, New Jersey 08544, USA

Felix Schlagintweit
Lerchenauerstrasse 167, D-80935 Munich, Germany

Martin Studeny†
Institute of Geology, Faculty of Geo- and Atmospheric Sciences, University of Innsbruck, A-6020 Innsbruck, Austria

ABSTRACT

The Cretaceous-Paleocene (K/P) boundary intervals are rarely preserved in successions of shallow-water limestones. Here, we describe a shallow rocky shore on the active orogenic wedge of the eastern Alps (Austria) fringed by a carbonate platform that was largely cannibalized by erosion. We compared this succession with similar nearshore environments globally, as well as the deep sea, to gain a better understanding of the environmental response to the K/P boundary transition. In the eastern Alps, Cretaceous and Paleocene lithofacies across the K/P boundary transition are separated by a hardground that formed during subaerial exposure and that terminates Upper Maastrichtian limestone with planktic foraminiferal assemblages deposited at neritic depth during zone CF3 (ca. 66.500 Ma). Above the hardground, there are beachrocks with early Danian zone P1a(1) assemblages, which indicate the hardground spans about ~600 k.y. of nondeposition and/or erosion. During the early Danian, the marine transgressive fringe fluctuated between "shoreface to emersion" environments, depositing limestones rich in bryozoans, rhynchonellids, coralline algae, and rare planktic foraminifera along with abraded, bored, and/or encrusted clasts eroded from older rocks. Repeated short subaerial exposure is marked by vadose diagenesis and hardgrounds, including an ~1.5 m.y. interval between magnetochrons C29n to C28n and planktic foraminiferal zones P1b to P1c(2).

*Diethard.G.Sanders@uibk.ac.at
†Current address: Biologiezentrum-Oberösterreichisches Landesmuseum, Johann-Wilhelm-Klein-Strasse 73, A-4040 Linz, Austria.

Sanders, D., Keller, G., Schlagintweit, F., and Studeny, M., 2019, Cretaceous-Paleocene transition along a rocky carbonate shore: Implications for the Cretaceous-Paleocene boundary event in shallow platform environments and correlation to the deep sea, *in* Adatte, T., Bond, D.P.G., and Keller, G., eds., Mass Extinctions, Volcanism, and Impacts: New Developments: Geological Society of America Special Paper 544, https://doi.org/10.1130/2019.2544(06).

Comparison with platform carbonate sequences from Croatia, Oman, Madagascar, Belize, and Guatemala, as well as nearshore siliciclastic environments of southern Tunisia, Texas, and Argentina, across the K/P boundary transition revealed surprisingly similar deposition and erosion patterns, with the latter correlative with sea-level falls and repeated subaerial exposure forming hardgrounds. Comparison with deep-sea depositional patterns revealed coeval but shorter intervals of erosion. This pattern shows a uniform response to the K/P boundary transition linked to climate and sea-level changes, whether in shallow nearshore or deep-sea environments, with climate change tied to Deccan volcanism in magnetochrons C29r-C29n.

INTRODUCTION

In shallow-water limestones, stratigraphically fairly complete Cretaceous-Paleocene (K/P) boundary intervals are rarely preserved because erosion and nondeposition resulted in major hiatuses that do not warrant in-depth study of the boundary transition. Consequently, shallow-water habitats are rarely documented and little understood with respect to the aftermath of the K/P boundary event. It is well known that Late Cretaceous biocalcifiers and other shelled biota became extinct (e.g., globotruncanids, rudists, ammonites, belemnites; e.g., Keller et al., 1996; Johnson et al., 2002; Steuber et al., 2002; Keller, 2005), whereas corals, red algae, bryozoans, and skeletal sponges survived without major diversity loss (Håkansson and Thomsen, 1999; Kiessling and Baron-Szabo, 2004; Sogot et al., 2013). Coral–red algal reefs flourished again at least during the middle to late Danian (Vecsei et al., 1998; Perrin, 2002; Baceta et al., 2005; Aguirre et al., 2007). However, shallow neritic environments are inherently prone to site-related effects such as differential subsidence, terrigenous input, shelf profile, substrate conditions, position along the shelf, and coastal upwelling. Despite these limitations, documentation of neritic K/P boundary transitions aids our understanding of the environmental consequences in nearshore habitats during the K/P boundary mass extinction.

In the eastern Alps of Europe, Paleogene synorogenic deep-water clastic units contain calciturbidites and debrites rich in clasts of Paleocene shallow-water limestones (Plöchinger, 1967; Lein, 1982; Tragelehn, 1996; Punekar et al., 2016). This led researchers to postulate that the active orogenic wedge was fringed by a Paleocene carbonate platform that was nearly completely cannibalized and redeposited in deep-water clastic sediments upon synorogenic deformation, uplift, and erosion (Tollmann, 1976; Wagreich and Faupl, 1994; Tragelehn, 1996). However, a shallow neritic K/P boundary interval is preserved on its original substrate only at the Kambühel location (Fig. 1; Plöchinger, 1967; Tragelehn, 1996). To date, the K/P boundary of Kambühel and particularly the sedimentology and biostratigraphy of the Danian interval remain unstudied.

Here, we report on the Kambühel location in the eastern Alps with a specific focus on lithofacies, biofacies, diagenesis, biostratigraphy, and depositional environment marked by a transgressive rocky shore overlain by beachrocks (Fig. 1). In order to better understand the effects of the K/P boundary mass extinction in very shallow platform environments, we compared the deposition and hiatus pattern from Kambühel with similar carbonate platform deposits from Croatia, Oman, Belize, and Guatemala and with nearshore siliciclastic K/P boundary sections from southern Argentina, Tunisia, and Texas. Finally, we compared the results from shallow-water environments with those from deep-sea sections to reveal differences and similarities across the K/P boundary transition from the late Maastrichtian through early Paleocene.

METHODS AND DEFINITIONS

The succession at Kambühel was mapped in light detection and ranging (LIDAR) orthoimages with 1 m isohypse resolution (1 m isohypsed LIDAR orthoimages are commercially available on demand from the government of Niederösterreich, Austria). Rock samples were extracted from vertical sections and from diverse outcrops (Table 1). More than 230 samples were examined in cut slabs, and 220 (4 × 6 cm) thin sections were used to document microfacies, diagenesis, and biostratigraphy. Outcrops are largely confined to low cliffs that fringe the brink of the mesa-like top of Kambühel (cf. Fig. 1C). Farther down section, a few natural exposures and outcrops along road cuts and paths permit thickness approximation of deeper-positioned lithostratigraphic units. LIDAR orthoimages combined with mapped stratigraphic units indicate that the Kambühel hill is cut by faults. Due to insufficient exposure and uncertainty regarding the potential syndepositional relief (see below), the faults could not be restored precisely. For this reason, the thicknesses indicated in the restored summary section (Fig. 2) are approximated. In contrast, the thickness of the Cretaceous-Paleogene boundary section was directly measured from a continuous vertical exposure (outcrop 2 in Fig. 1C; Table 1).

We attempted to deduce the original polymorphy of isopachous fibrous cements that represent widespread initial diagenetic precipitates of lower Danian grainstones. The rationale was that if these cements were originally aragonite, they might have retained elevated Sr concentration; conversely, if they originally were magnesium calcite, an elevated Mg concentration would be expected (cf. Tucker and Wright, 1990; James and Jones, 2016). We carefully selected four samples of well-preserved fibrous cement and tested them with electron probe microanaly-

sis (EPMA). The samples showed no Sr and Mg concentrations beyond analytical uncertainty. EPMA measurements were done on a JEOL JXA-8100 with 5 wavelength-dispersive spectrometers and a SUN-BLADE Workstation with a Solaris (UNIX) operating system and a resolution of ~10 eV. The acceleration voltage was 15 kV, the probe current was 10 nA, and the sample diameter was 20 µm. For Mg determination, the Kα emission line and 50 s measurement time were chosen; for Sr, the Lα emission line and 50 s of measurement time were chosen. Furthermore, element mapping done on two selected thin sections with

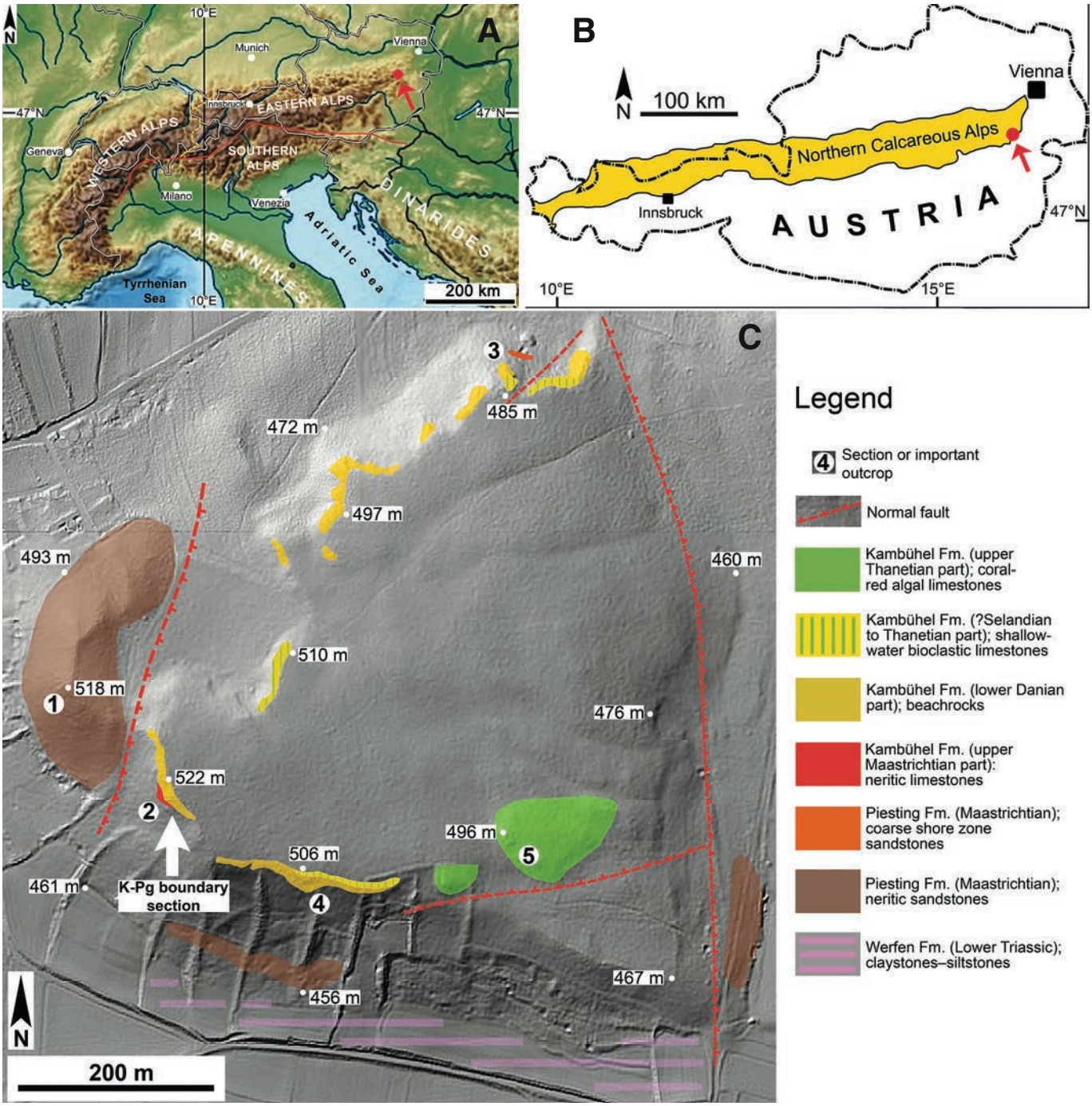

Figure 1. (A, B) Position of Kambühel in the European Alps (A) and at the eastern fringe of the Northern Calcareous Alps of Austria (B). (C) Light detection and ranging (LIDAR)–based geological map of Kambühel hill, with Cretaceous-Paleogene boundary (K-Pg; section number 2) and other important sections indicated. Most of the hill consists of an Upper Maastrichtian to Upper Thanetian succession that is gently tilted toward the east and cut by normal faults.

TABLE 1. LOCATION OF SECTIONS SHOWN IN FIGURE 1C AND THEIR SIGNIFICANCE

Section number	Coordinates	Lithostratigraphic affiliation; age range
1	47°44′47.57′N, 16°1′40.47′E	Piesting Formation; Upper Maastrichtian
2	47°44′45.97′N, 16°1′45.32′E	**Cretaceous-Paleogene boundary section** Kambühel Formation *pro parte;* Upper Maastrichtian to Danian
3	47°44′58.26′N, 16°2′00.22′E	Kambühel Formation *pro parte*; Danian to Thanetian
4	47°44′42.45′N, 16°1′51.87′E	Kambühel Formation *pro parte*; Danian to Thanetian
5	47°44′44.93′N, 16°1′55.11′E	Kambühel Formation *pro parte*; Upper Thanetian

Note: See also Figure 2 for reconstructed succession and vertical position of sections.

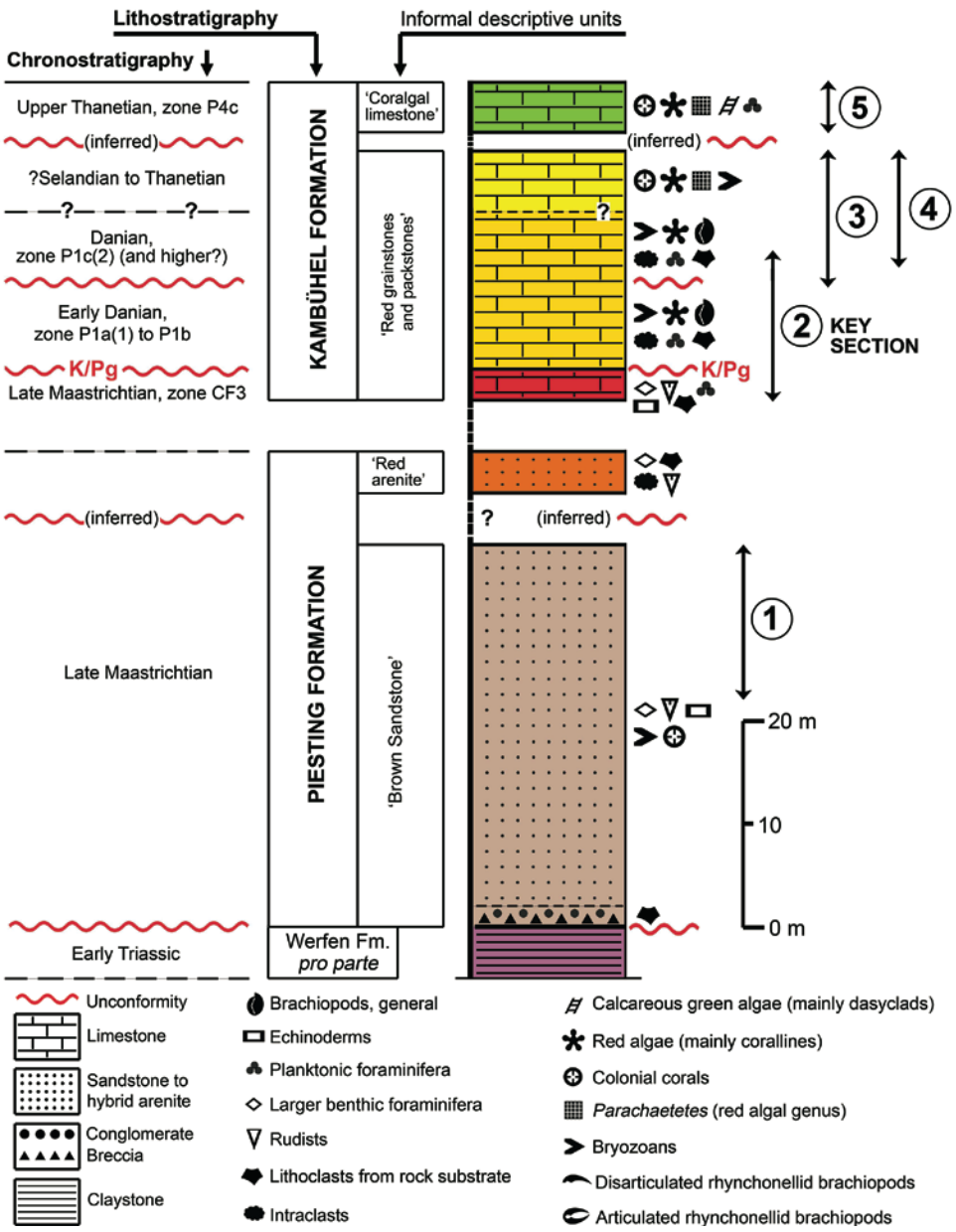

Figure 2. Restored summary section at Kambühel. Because of faulting and limited exposure, the total thicknesses of stratigraphic units are estimates. Chronostratigraphic assignments are based on biostratigraphic data. Overlapping portions of sections 2–4 (cf. Fig. 1C) were deduced from similarities in sedimentary facies and from biochronostratigraphy. The positions of sections 3 and 4 could not be determined precisely and are estimates. See text for further description. K/Pg—Cretaceous-Paleogene boundary.

isopachous fibrous cements (not identical to the thin sections used for EPMA) showed that Sr and Mg were not significantly elevated above background. Element mapping was done in low-vacuum mode on a digital scanning microscope JEOL JSM-5130LV at 15 kV acceleration voltage with an energy-dispersive electron detector, a gun current of 5 μA, and a spot size of 55 μm. The implications of these results are discussed below.

Hereafter, the term "hybrid arenite" designates a grain-supported sediment mainly of sand-sized grains of siliciclastic, carbonate-lithic, and bioclastic composition of highly variable relative mixtures (cf. Zuffa, 1985; Haldar and Tisljar, 2014). In hybrid sandstones, the siliciclastic sediment fraction prevails over the other two fractions.

GEOLOGICAL SETTING

In the domain of the future eastern Alps, Early Cretaceous stacking of fold-and-thrust nappes was followed by uplift and erosion of the accretionary wedge. From the Turonian onward, the nappe stack was onlapped and overstepped by a synorogenic succession termed the Gosau Group (Wagreich and Faupl, 1994; cf. Platt, 1986), which consists of a lower subgroup of terrestrial to neritic deposits separated by an unconformity from the upper subgroup consisting mainly of deep neritic to bathyal deposits (Wagreich and Faupl, 1994; Sanders et al., 1997). The Northern Calcareous Alps (Fig. 1B), which consist of a nappe stack dominated by Triassic shallow-water carbonates, host large erosional relicts of the Gosau Group. The Late Cretaceous to Eocene depositional setting of the Gosau Group was located at ~30°N–32°N. During Gosau deposition, the eastern Alpine domain was a northward-dipping orogenic wedge crowned by one or more forested islands (cf. Handy et al., 2015). Microtidal shelves were dominated by waves and storms (Sanders, 1998; Sanders and Höfling, 2000). An overall subtropical environment is indicated by build-ups of corals and/or rudists (see Darga, 1990; Sanders and Baron-Szabo, 1997; Sanders and Pons, 1999).

In the internal part of the orogenic wedge, metamorphic rocks were exhumed and supplied siliciclastic detritus. Deposition of shallow-water limestones was confined to inner shelves sheltered from terrigenous input. These limestones accumulated from deposystems that consisted of, in a seaward direction: (1) protected shallow subtidal areas (lagoons), (2) bioclastic sand bodies subject to high-energy events, and (3) coral-rudist build-ups (Sanders and Höfling, 2000). Another significant limestone deposystem, which includes the Kambühel section, was represented by wave-dominated shore zones struck by episodic high-energy events. The records of these typically transgressive shores are up to ~15 m thick and mainly consist of carbonate lithoclasts mixed with abraded-bioeroded bioclasts of penecontemporaneous marine habitats (e.g., benthic foraminifera with stout tests, bryozoans, rhynchonellid brachiopods, coralline algae, and, rarely, a few rudists and colonial corals). In the Cretaceous part of the Gosau Group, these shore-zone successions coexisted with coral-rudist–dominated deposystems elsewhere (Sanders, 1998; Sanders and Höfling, 2000). Lack of tidal flats of siliciclastic or carbonate type, sedimentological evidence for wave/storm-dominated shore zones, and the tectonic setting on an active margin all suggest that the Gosau shelves were comparatively narrow and steep (Wagreich and Faupl, 1994; Sanders and Höfling, 2000; Wagreich, 2001).

RESULTS

Lithostratigraphy and Biostratigraphy

The base of Kambühel hill consists of poorly exposed Lower Triassic siltstones to claystones of the Werfen Formation (Table 2), which unconformably underlie the Piesting Formation of the Gosau Group; the latter formation variably spans from the late Campanian to late Maastrichtian due to syntectonic deposition (Figs. 1C and 2; Table 2; cf. Piller et al., 2004). At the Kambühel hill, the base of the Piesting Formation consists of breccias to shore-zone conglomerates, but most of the formation is a dark-brown–weathered, fossiliferous hybrid sandstone representing neritic environments (brown sandstone unit in Fig. 2; Table 2).

Section 1 up to the top of the brown sandstone unit shows little variation in composition, texture, and bioclasts. The larger benthic foraminiferal assemblage (e.g., *Siderolites calcitrapoides*, *Sirtina ornata*) indicates that at least the middle to upper part of the Piesting Formation is of late Maastrichtian age (see Table 2). Above a gap in exposure related to faulting, the brown sandstone unit is overlain by poorly sorted, red-weathered, coarse sandy hybrid arenites with admixed bioclasts from neritic environments (Red arenites in Fig. 2; Table 2). In this unit, abundant intraclasts and strongly fragmented and abraded/bored bioclasts indicate reworking, either during forced regression or during transgressive reworking after a relative sea-level fall (Table 2). No evidence was found to distinguish between these possibilities. In any case, we infer that this unit is underlain by an unconformity (Fig. 2).

The overlying Kambühel Formation consists mainly of limestones that are monotonously light-red to dark-red, indistinctly thick-bedded grainstones and packstones (Red grainstones and packstones in Fig. 2). These limestones are rich in strongly fragmented, abraded, microbored, and encrusted bioclasts (Fig. 3). These largely reworked fossils were probably derived from a transgressive shoreface and were admixed to a parautochthonous neritic bioclast spectrum consisting mainly of larger benthic foraminifera, bryozoans, and planktic foraminifera (Table 2). The oldest part of the Kambühel Formation is exposed in section 2, which contains the K/P boundary (Figs. 1C, 2, and 4). The basal part of section 2 consists of bioturbated packstones rich in late Maastrichtian larger benthic and planktic foraminifera (Schlagintweit et al., 2016). The robust planktic foraminiferal index species *Pseudoguembelina hariaensis* spans the Upper 191 Maastrichtian zone CF3, equivalent to magnetochron C30n and zones CF2–CF1, equivalent to C29r below the K/P boundary (Keller, 2014).The rest of the planktic foraminiferal assemblage consists of low-diversity, large, complex species with robust

TABLE 2. STRATIGRAPHIC UNITS, BIOCHRONOSTRATIGRAPHY, AND INTERPRETATION OF SUMMARY SECTION AT KAMBÜHEL (FIG. 2)

Formation; *informal subdivision*	Lithologies	Texture, bioclasts, and other features	Important index fossils; age	Interpretation, figure reference
Piesting Formation (PFm) *Brown sandstone* unit	Bioturbated, fine- to medium-grained hybrid arenites, mainly of quartz, carbonate-lithic grains, and bioclasts	Smaller benthic foraminifera, larger benthic foraminifera, colonial corals, rudists, red algae, brachiopods, echinoids, coralline algae, bryozoans	*Siderolites calcitrapoides*, *Sirtina ornata*, *Lepidorbitoides*, *Orbitoides* (with large embryonic chambers), *Praestorrsella roestae* Late Maastrichtian	Sandstone of normal-marine neritic setting; corals, rudists, and brachiopods were transported to site by episodic high-energy events
Piesting Formation (PFm) *Coarse red arenite* unit	Red, stylobedded coarse hybrid arenites, mainly of quartz, rock fragments, carbonate-lithic grains, and bioclasts	Bioclast fraction mainly of fragmented larger benthic foraminifera; bioclasts abraded and bored; arenite lithified by intergranular pressure solution and stylolitization	Fragments of larger benthic foraminifera as above, probably all reworked Late Maastrichtian *pro parte* (per implication from underlying and overlying intervals)	(a) Forced regressive nearshore deposit, or (b) shore zone deposit formed by transgressive reworking
Kambühel Formation (KFm) Upper Maastrichtian portion of formation	Red, faintly thick- and wavy-stylobedded limestones with a few percent of siliciclastic grains and rounded lithoclasts of Werfen Formation	Bioturbated bioclastic packstones rich in larger benthic foraminifera, bilaminate and branched bryozoans, corallines, smaller benthic foraminifera Bioclast preservation ranges from complete to fragmented, abraded, bored, and encrusted	Planktonic foraminifera: *Pseudoguembelina hariaensis*, *Planoglobulina brazoensis*, *Planoglobulina carseyae*, *Contusotruncana contusa*, *Globotruncana arca*, *Globotruncana depeublei*, *Globotruncanella petaloidea*, *Gansserina gansseri* Larger benthic foraminifera: *Siderolites calcitrapoides, Orbitoides brinkae, Lepidorbitoides socialis, Hellenocyclina beotica, Sirtina ornata, Daviesina fleuriausi, Clypeorbis? ultima* (Schlagintweit et al., 2016) Late Maastrichtian zone Cretaceous foraminifer zone 3 (CF3) *Pseudoguembelina hariaensis* (Keller, 2014)	Limestone of neritic environment of moderate water energy; significant input of reworked bioclasts and lithic grains (perhaps from a transgressive shore zone) during high-energy events (Figs. 3 and 7)
Cretaceous-Paleocene boundary hardground (Figs. 8, 9, 10, and 14) Hiatus: late Maastrichtian CF3 biozone *pro parte* to early Danian P1a(1) biozone *pro parte* Estimated hiatus duration: ~700 k.y. (cf. Keller, 2014; Berggren and Pearson, 2005)				
Kambühel Formation (KFm) Danian part of formation	Red, indistinctly stylobedded limestones with a few percent of siliciclastic grains	Grsts (less commonly pksts) of fragments of branched bryozoans, red algae, intraclasts; bio/intraclasts abraded, bored, encrusted; grsts with fenestral pores; grsts lithified by isopachous fringes of fibrous cement and/or by micritic meniscus and pendant cements	Planktonic foraminifera: *Chiloguembelina midwayensis*, *Woodringia hornerstownensis*, *Guembelitria cretacea*, *Parasubbotina pseudobulloides*, *Subbotina trioloculinoides* Benthic foraminifera: *Solenomeris* sp., *Stomatorbina binkhorsti*, *Cibicidoides* gr. *succedens*, *Planorbulina uva*, polymorphinids Hiatus within Danian: Early to late Danian *pro parte*, zone P1a(1) to P1c(2) after Berggren and Pearson (2005)	Grst package represents stacked beachrock units; bioclast fraction results from (1) hard-substrate shore zone habitat, (2) influence of cooler/high-nutrient waters (coastal upwelling), combined with (3) taphonomic bias for bryozoans (Figs. 11 and 12) See Fig. 13 for intra-Danian hardground
Kambühel Formation (KFm) ?Selandian to Thanetian part of formation	Red weathered, indistinctly stylobedded limestones with accessory siliciclastics	Package of grsts similar to Danian part of succession, but fringes of fibrous cement and micritic cements rare, mainly cemented by calcite spar	Benthic foraminifera: *Rotorbinella* cf. *hensoni*, *Planorbulina uva-cretae, Stomatorbina binkhorsti* Package unclear with respect to precise biochronostratigraphic delimitation	Grsts accumulated in a nearshore setting, farther offshore than the Danian limestones

(*Continued*)

TABLE 2. STRATIGRAPHIC UNITS, BIOCHRONOSTRATIGRAPHY, AND INTERPRETATION OF SUMMARY SECTION AT KAMBÜHEL (FIG. 2) (*Continued*)

Formation; *informal subdivision*	Lithologies	Texture, bioclasts, and other features	Important index fossils; age	Interpretation, figure reference
Kambühel Formation (KFm) Upper Thanetian part of formation	Red-gray to gray, indistinctly thick-bedded limestones	Poorly sorted shallow-water bioclastic floatstone to bafflestone with colonial corals, *Parachaetetes*, calcareous green algae, red algae; corals and *Parachaetetes* may show complex encrustation successions	Planktonic foraminifera: *Globanomalina pseudomenardii, Globanomalina imitata, Globanomalina chapmani, Acarinina soldadoensis, Acarinina coalingensis, Subbotina triangularis, Subbotina velascoensis, Morozovella apanthesma, Morozovella acuta* Benthic foraminifera: *Cocoarota orali*, *Stomatorbina* sp., *Haddonia praeheissigi*, *Planorbulina cretae* Upper Thanetian *pro parte* (zone P4c after Berggren and Pearson, 2005)	Normal-marine, shallow subtidal, subtropical carbonate environment subject to episodic high-energy events

Note: Names of formations are according to the Stratigraphic Chart of Austria (Piller et al., 2004). Abbreviations: grst—grainstone; pkst—packstone.

shells able to survive in shallow nearshore environments (Figs. 5 and 6; Table 2).

Maastrichtian CF3 limestones are topped by the K/P boundary hardground (Figs. 2 and 4). Above this hardground, reworked Cretaceous foraminifera are common as isolated specimens (typically more-or-less fragmented, abraded, and/or bored) and in clasts. Danian planktic foraminifera are present in the matrix between clasts and occasionally within clasts. The oldest Danian biozone identified is the upper part of zone P1a(1) (biozonation by Keller et al., 1996, 2002), which spans from the first appearance of *Parvularugoglobigerina eugubina* to the first appearances of *Parasubbotina pseudobulloides* and/or *Subbotina triloculinoides* (Fig. 5). The major part of the Kambühel Formation consists of Danian limestones (Figs. 1C and 2).

The most widespread facies consist of grainstones that became cemented by an isopachous fringe of fibrous cement, or micritic

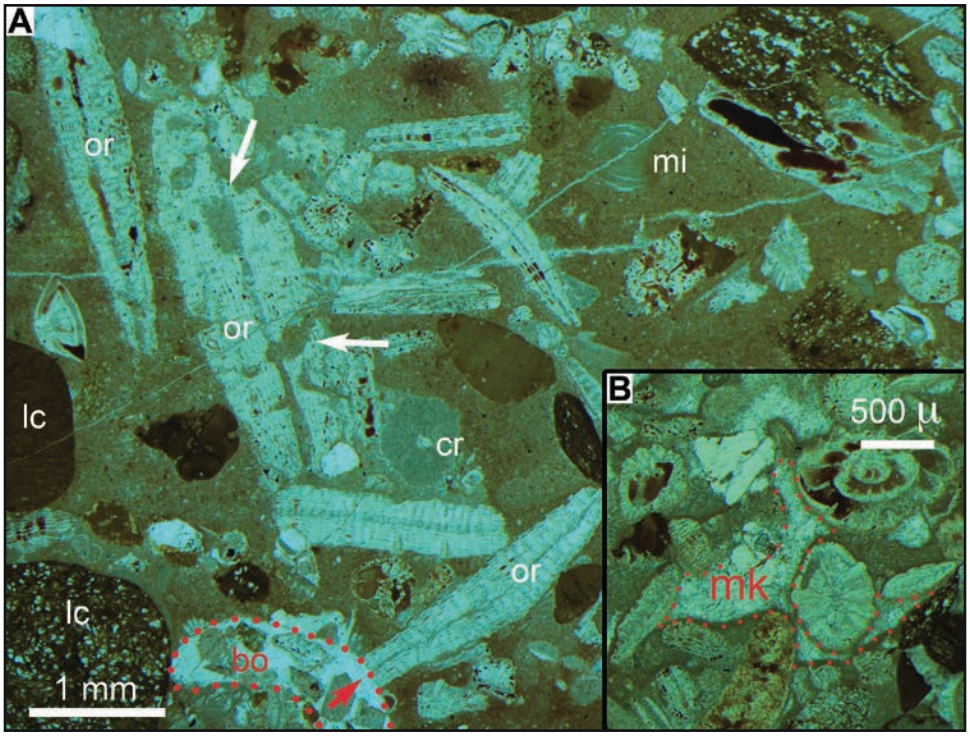

Figure 3. (A) Bioturbated bioclastic packstone composed mainly of fragmented, abraded, and bored (white arrows) orbitoid larger benthic foraminifera (or), crinoid ossicles (cr), and a miliolid foraminifer (mi). Brownish components (lc) are lithoclasts from the local rock substrate (Werfen Formation; see Table 1). Note truncation (red arrow) of orbitoid foraminiferal test along the margin of a boring (bo, outline stippled red). Parallel nicols. (B) Detail of same type of packstone as shown in preceding image. Note microkarstic dissolution pore (mk, outline stippled red) filled with blocky calcite spar. Parallel nicols (µ—µm).

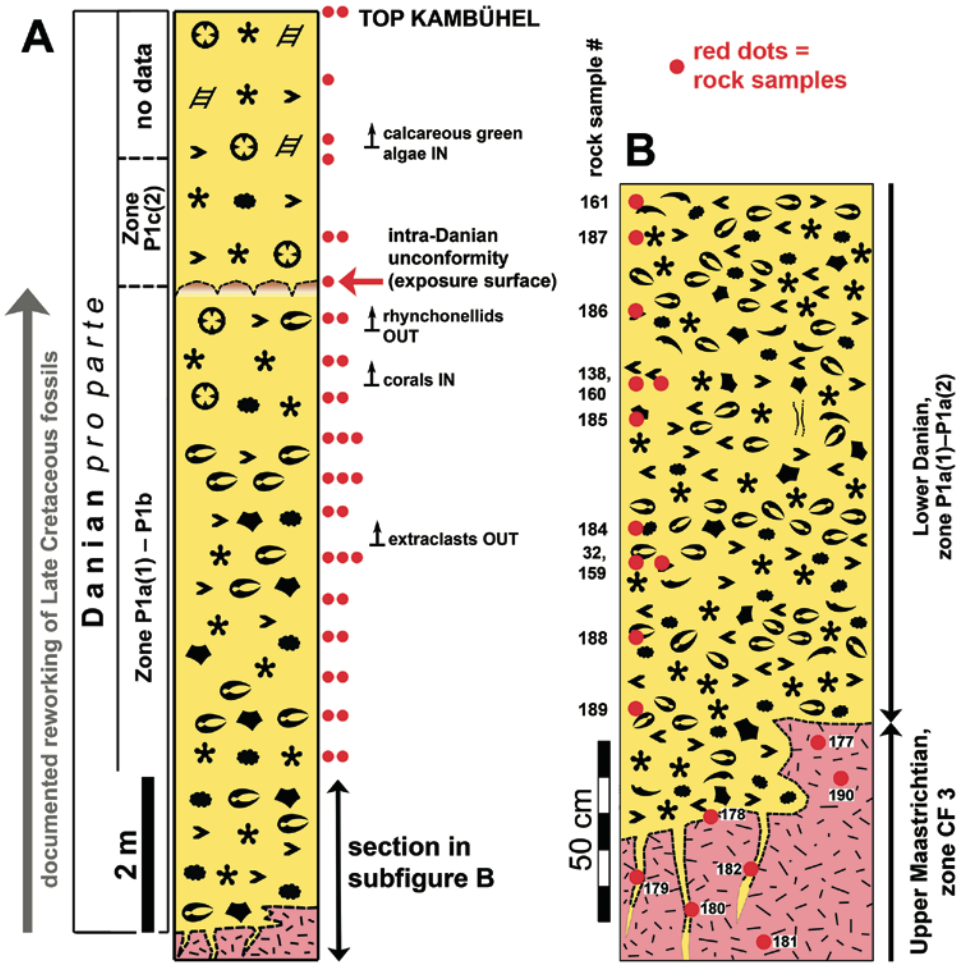

Figure 4. (A) K/P boundary section at location 2 (Table 1; Fig. 1C; see Fig. 2 for symbols). The entire succession consists of limestone. (B) Detail of K/P boundary with sample numbers. CF—Cretaceous foraminifera.

meniscus and pendant cements. Typical components include coralline algae, bryozoans, common rhynchonellid brachiopods (e.g., section 2), intraclasts, and lithoclasts (Table 2). About 2 m above the K/P boundary hardground (section 2), a more diverse assemblage of 10 identified planktic foraminiferal species marks zone P1a(2), with the top of this zone identified by the last appearance of *P. eugubina,* which is equivalent to the top of magnetochron C29r (Fig. 6). Above this interval, there is a second Danian hardground that contains an impoverished and poorly preserved planktonic foraminiferal assemblage of zone P1b, equivalent to C29n (Figs. 4A and 6). Above the intra-Danian hardground, only a few planktic foraminifera are present, including the index species *Praemurica inconstans*, which marks the upper half of zone P1c(2). This suggests dissolution, nondeposition, and abrasion effects, as also indicated by a persistent content in reworked Cretaceous species up to the hardground (Figs. 4A and 5).

At two locations, Danian limestones are overlain by a few meters of grainstones deposited during the ?Selandian–Thanetian interval (Figs. 1C and 2). The bioclast content of the grainstones is similar to those of Danian limestones, but large fragments of colonial corals and the red alga *Parachaetetes* are also common (Fig. 2; Table 2). Along the base of the ?Selandian–Thanetian unit no clear-cut boundary surface or sharp facies change was identified. Near the southeastern corner of the Kambühel hill, a unit of floatstones, bafflestones, and rudstones is exposed with branched corals, massive and foliose corals, *Parachaetetes*, coralline algae, and hydrozoans (Fig. 1C; coralgal limestones in Fig. 2). The matrix consists of bioclastic wackestone to packstone with smaller benthic foraminifera (*Miliolina*, *Textularina*, *Rotaliina*), fragments of diverse dasycladaleans, and planktonic foraminifera. Globorotaliids allow for identification of the Upper Thanetian (P4c biozone; Table 2).

Sediment textures and fossils in the coralgal limestones record deposition in shallow subtidal, normal-marine environments struck by episodic high-energy events (Table 2). The coralgal limestones unit most probably overlies an unconformity, as suggested by the different facies contents and late Thanetian age. The entire Lower Danian to Upper Thanetian succession is no more than a few tens of meters thick (Fig. 2) and consists entirely of shore-zone to protected shallow-subtidal facies, which include at least two hiatuses, with the missing intervals fairly well constrained. This indicates that the Kambühel Formation is rich in stratigraphic gaps related to intermittent subaerial exposure and sea-level fluctuations.

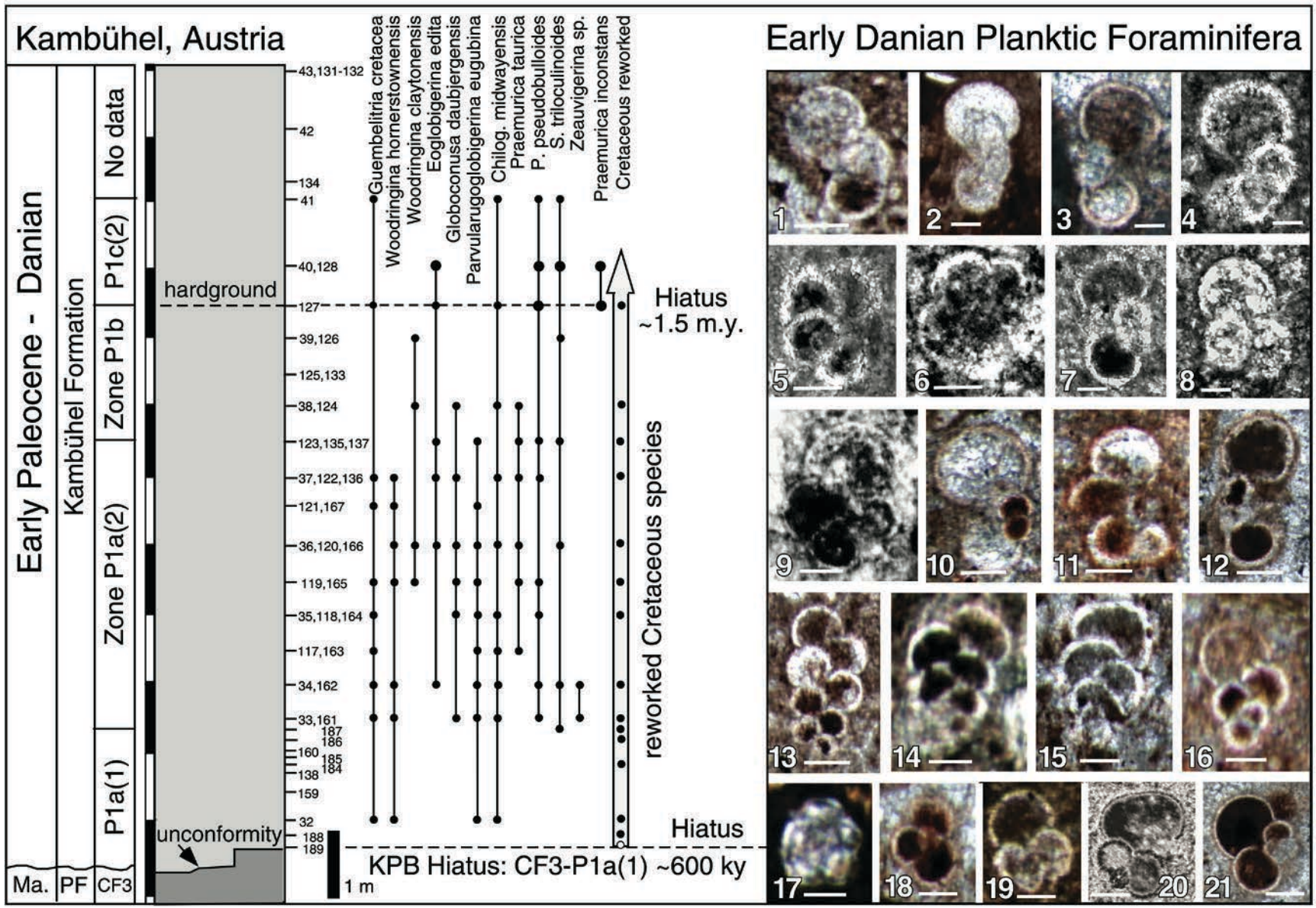

Figure 5. Summary of biostratigraphic data in section 2 (cf. Figs. 1C and 2), based on planktic foraminifera identified from thin sections. Biozonation is based on Keller et al. (1996, 2002). Black circles mark Danian species occurrences; black circles in arrow mark reworked Cretaceous species. KPB—K/P boundary. (1) *Eoglobigerina edita* (Subbotina). (2, 3) *Parasubbotina pseudobulloides* (Plummer). (4) *Praemurica inconstans* (Subbotina). (5, 6) *Praemurica taurica* (Morozova). (7–10) *Subbotina triloculinoides* (Plummer). (11, 12) *Parasubbotina pseudobulloides* (Plummer). (13) *Woodringina hornerstownensis* Olsson. (14) *Chiloguembelina morsei* (Kline). (15) *Chiloguembelina midwayensis* (Cushman). (16) *Woodringina claytonensis* Loeblich and Tappan. (17) *Parvularugoglobigerina eugubina* (Luterbacher and Premoli Silva). (18, 19) *Guembelitria cretacea* Cushman. (20, 21) *Globoconusa daubjergensis* (Brönnimann). Scale bar = 50 µm. PF—planktic foraminifera; CF—Cretaceous foraminifera.

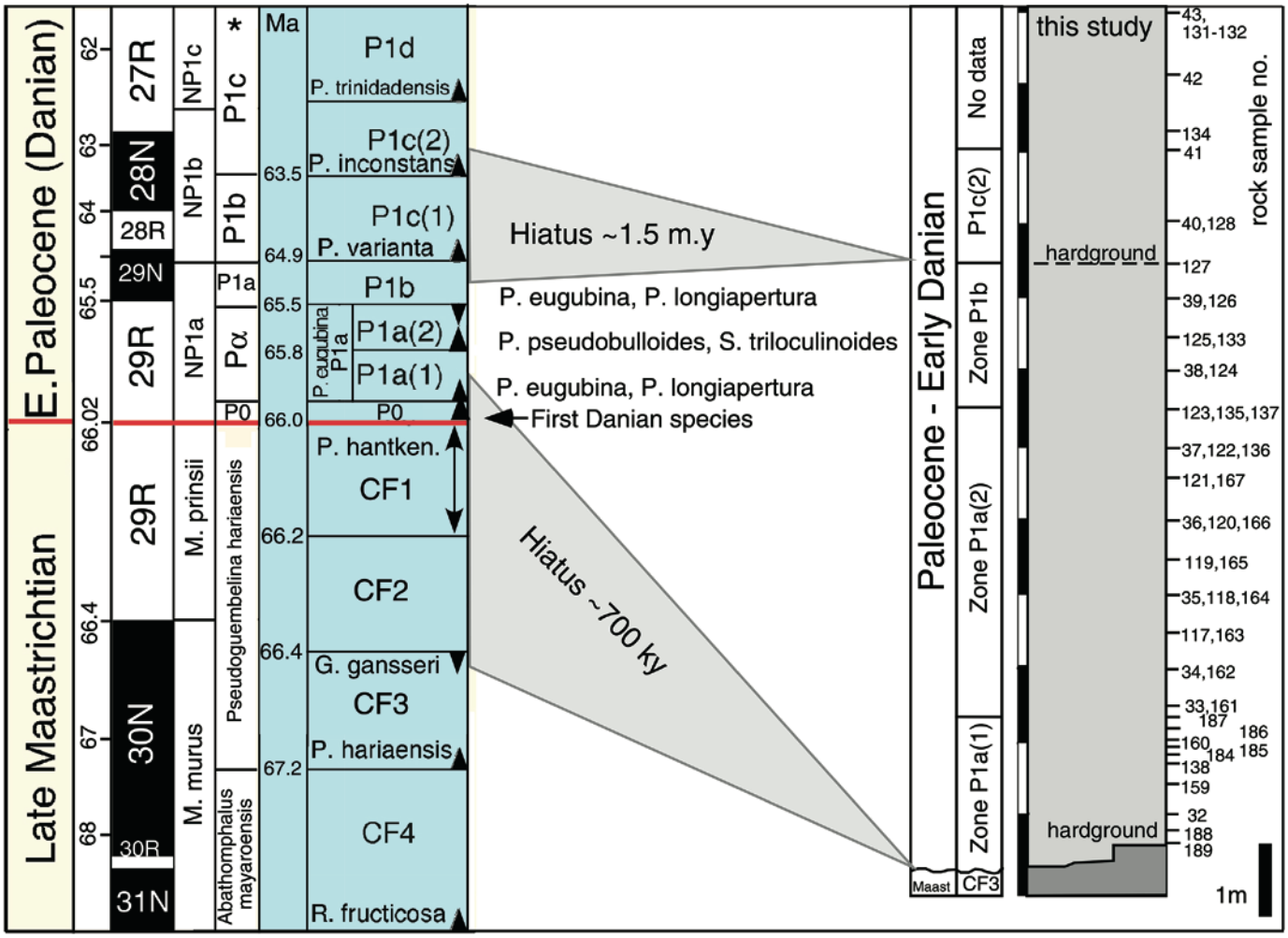

Figure 6. Chronostratigraphy (in Ma) of section 2 based on planktonic foraminiferal zonal schemes by Keller et al. (1996, 2002) for the early Danian, and Li and Keller (1998a, 1998c) for the Maastrichtian. Shown for comparison are other planktic foraminiferal zonal schemes (Olsson et al., 1999; Berggren and Pearson, 2005; Huber et al., 2008) and nannofossils (Burnett, 1998). Two hardgrounds mark hiatuses: one across the Cretaceous-Paleogene boundary (KPB) with an estimated 600 k.y. missing, and the other in the late Danian between zones P1b and P1c(2) with ~1.5 m.y. missing. CF—Cretaceous foraminifera. Key to foraminiferal genera: *Praemurica trinidadensis*, *Praemurica inconstans*, *Parasubbotina varianta*, *Parvularuglobigerina eugubina*, *Parvularuglobigerina longiapertura*, *Parasubbotina pseudobulloides*, *Subbotina triloculinoides*, *Plummerita hantkeninoides*, *Gansserina gansseri*, *Pseudoguembelina hariaensis*, *Racemiguembelina fructicosa*. Key to nannofossil genera: *Micula murus*, *M. prinsii*.

Estimates of Hiatus Duration

The ages and durations of hiatuses and hardground formation can be estimated based on correlation of biostratigraphy (biozone ages) with magnetostratigraphy and cyclostratigraphy calibrated with U-Pb geochronology. High-precision U-Pb zircon dating of the Deccan Traps in India yielded a 65.552 ± 0.026 Ma age for the top and 66.288 ± 0.027 age for the base of C29r, for a total duration of 736 ± 37 k.y. (Schoene et al., 2015). The K/P boundary is currently placed at ca. 66.021 ± 0.024 Ma, based on U-Pb dating in the Denver Basin, Colorado (Clyde et al., 2016), and recalculated at 65.970 ± 0.030 Ma. This suggests that C29r below the K/P boundary spans a maximum of 345 k.y., which is within the error margin of the ~350 k.y. derived from orbital cyclostratigraphy estimates in marine sections (Sinnesael et al., 2016; Thibault and Husson, 2016; Thibault et al., 2016). Differences in cyclostratigraphy of marine sections are generally due to the number of cycles present (16 vs. 18), with the lower number likely due to K/P boundary section erosion, as suggested by the frequent absence of the topmost Maastrichtian rapid global warming that spans ~40 k.y. or two cycles (Thibault et al., 2016).

The duration of planktic foraminiferal zones CF1 and CF2 spans from the upper C30n magnetochron to the K/P boundary. Their ages based on cyclostratigraphy of the auxiliary stratotype section at Elles, Tunisia, reveal that zone CF1 spans the last

200 k.y. of the Maastrichtian ending at the K/P boundary, whereas zone CF2 spans the preceding 250 k.y. (Thibault et al., 2016). This entire interval is missing at Kambühel below the K/P boundary. In the early Danian, zones P0, P1a(1), and P1a(2) correspond to C29r above the K/P boundary, spanning ~420 k.y. (65.552 ± 0.026 Ma to 65.970 ± 0.030 Ma). At Kambühel, the missing interval spans zones P0 and most of P1a(1), or about ~150 k.y. The K/P boundary hiatus thus spans at least 600 k.y.

The preserved Danian part of the Kambühel Formation accumulated during an interval of time corresponding to the upper part of P1a(1) into zone P1b (Figs. 5 and 6). Age estimates for the overlying intra-Danian hardground (Figs. 4 and 6) can be derived from correlation of biozones to magnetostratigraphy (Olsson et al., 1999; Berggren and Pearson, 2005). Based on this age scheme, the hiatus spans from the upper zone P1b into the upper zone P1c(2), or about ~1.5 m.y. (Fig. 6; Table 2). This implies that the maximum age of the Danian interval represented at Kambühel is ca. 3.2 Ma, and at least half of this interval is missing due to nondeposition and erosion. Another Paleocene hiatus is inferred toward the topmost late Thanetian part (Coralgal limestones) of the Kambühel Formation (Figs. 1 and 2; Table 2).

Lithology of the K/P Transition

At Kambühel, Upper Maastrichtian limestones below the K/P boundary are gray- to red-colored, bioturbated bioclastic packstones with a wide spectrum of bioclasts from neritic environments rich in benthic foraminifera (Table 2). Many bioclasts are broken, abraded, and bioeroded (Fig. 3). In addition, rounded clasts of light-brown siltstone to claystone from the underlying Lower Triassic Werfen Formation are common. Backscattered-electron element mapping indicated that the typical brown stain of the clasts is related to iron, probably iron oxides (goethite, limonite). Maastrichtian limestones are riddled with a system of cavities varying from 1 mm to a few centimeters in width and at least 6–12 cm in vertical extent (height of polished rock slabs; Fig. 7). Locally, the margins of the cavities are coated by a thin crust of dark-brown iron oxide (Fig. 7D). In the centimeter-thick margin

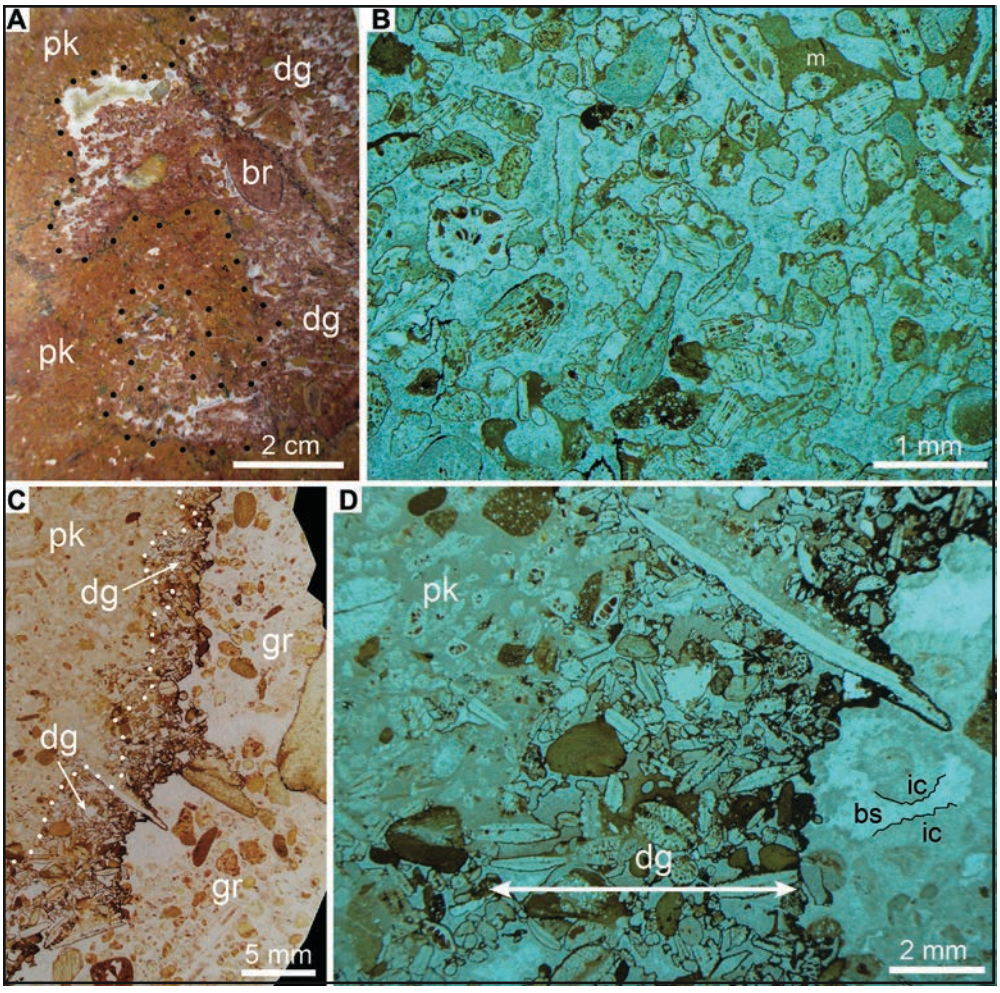

Figure 7. (A) Upper Maastrichtian packstone (pk) with a cavity (outline stippled black) filled with diagenetic grainstone (dg). Note articulated brachiopod shell (br) filled with bioclastic packstone. Kambühel Formation (Upper Maastrichtian part). Reflected light photo of polished slab. (B) Thin section of diagenetic grainstone that fills the cavity shown in preceding image. Except for a few small remnants (m), the original matrix of lime mudstone was dissolved away; only bioclasts and lithoclasts remained. The grains show a thin fringe of brownish micrite; locally, micritic meniscus cements are present. The secondary pore space is largely filled by an isopachous fringe of cement. Parallel nicols. (C) Upper Maastrichtian bioclastic packstone (pk), cut by a cavity filled with Danian grainstone (gr) mainly of lithoclasts and fragments of coralline algae and bryozoans. Note the rugged cavity margin outlined with brown, iron-oxide staining, and the "halo" of diagenetic grainstone (dg, outline stippled white) along the contact. Reflected light photo of thin section. (D) Thin section detail of preceding image. Toward the cavity, the Maastrichtian larger benthic foraminiferal packstone (pk) grades into a diagenetic grainstone (dg) with interstitial matrix dissolved out. Note blackish iron-oxide staining along the cavity margin. The cavity is filled with Danian grainstone that is cemented by a thick, isopachous fringe of radial-fibrous cement (ic); remnant pore space became filled by blocky calcite spar (bs). Translucent light, parallel nicols.

surrounding the cavities, the host packstone is riddled with open pores between bioclasts. These pores commonly show complex, variable infillings, including (1) geopetal fabrics of lime mudstone, often in several layers separated by red- or brown-stained surfaces of irregular shape, (2) isopachous fringes of cement, (3) crystallized silt, and (4) micropeloidal grainstones (Fig. 7D).

The cavities are most commonly filled with poorly sorted Lower Danian litho-bioclastic grainstones to packstones rich in bryozoan fragments, with rhynchonellid brachiopods, and with common intraclasts of Lower Danian bryozoan limestones. Bioclasts and intraclasts range in preservation from fresh and unaltered to more commonly abraded, rounded, microbored, and/or encrusted. Lower Danian limestones in cavities are riddled with fenestral pores, vugs, and fractures that show complex infillings (e.g., cement fringes, geopetally laminated lime mudstone, grainstone). In addition, geopetally laminated, red to pink lime mudstone to lithic wackestones to packstones show infillings occasionally cut by irregular dissolution surfaces, followed by renewed infillings of fine-grained carbonate sediments.

K/P Boundary Hardground

A hardground with complex morphology separates the Upper Maastrichtian and Lower Paleocene Danian sediments (Fig. 8).

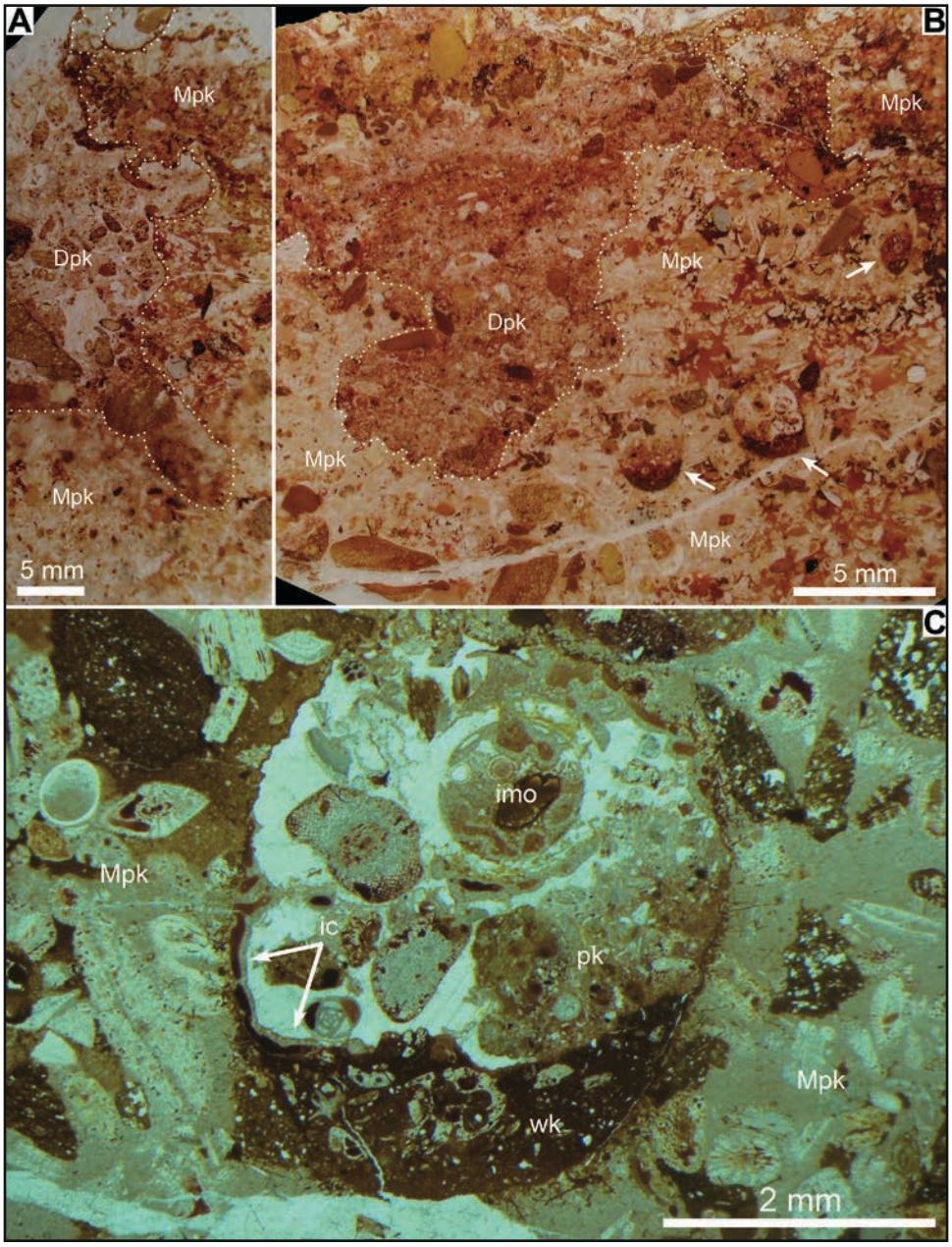

Figure 8. (A, B) K/P boundary hardground: Irregular, rugged surface (white stipples) between Upper Maastrichtian larger foraminiferal packstone to diagenetic grainstone (Mpk) and Lower Danian litho-bioclastic packstone (Dpk) above. Reflected-light thin section photographs. In B, note macroborings (white arrows) of subcircular cross section. (C) Detail of one of the macroborings shown in B. The boring shows an infilling of brown bioclastic wackestone (wk), sharply overlain by bioclastic packstone (pk); later dissolution produced secondary interstitial pore space between bioclasts, resulting in diagenetic grainstone. Note internal mold (imo), probably after a microgastropod. The pore space became filled with an isopachous fringe of radial-fibrous cement (ic) and, mainly, by blocky calcite spar (translucent). Note irregular rugged margin of macroboring. Parallel nicols.

The hardground surface is marked by delicate millimeter-scale projections excavated from Upper Maastrichtian bioclastic packstone, as well as cuspate and convex-concave projections and recesses ranging from 1 mm to a few centimeters in width; deeper recesses of the hardground are overlain by Danian packstone (Fig. 9). Up section and along higher-projecting intervals of the hardground, the packstone is overlain by Danian grainstone rich in coralline-algal and bryozoan fragments. In polished slabs and thin sections, the hardground shows a vertical relief of ~3 cm (Fig. 10). However, the local vertical relief in the field ranges up to a few decimeters over a lateral distance of a few meters. Rock samples from similar elevation in the K/P boundary interval consist of Maastrichtian limestones (some riddled with cavities), exposed K/P boundary hardground (two samples), and Lower Danian limestones (Figs. 4B and 7). This indicates a highly irregular hardground surface.

Lower Danian

Textures and Component Spectrum

Lower Danian limestones range from very poorly to well-sorted grainstones to fine-grained rudstones (see Table 3A). Many grainstones show fenestral pores and/or characteristic sparse packing of components. Grainstones mainly consist of: (1) abraded and microbored fragments of bryozoans and corallinaceans, vertically and laterally poorly delimited levels rich in the rhynchonellid *Basilicocostella* (Dulai et al., 2008), and, to a lesser extent, smaller benthic foraminifera (rotaliines, miliolids) and planktic foraminifera; (2) lithoclasts derived from older substrate rocks (Werfen Formation; Table 2); and (3) first- and second-cycle intraclasts frequently consisting of bored and/or encrusted grainstones to packstones with components identical to the Danian host grainstone or Upper Maastrichtian limestone (Fig. 11). The bryozoan fauna consists of Cheilostomata and Cyclostomata, with representatives of both groups grown in erect positions and delicately branched, which probably required hard substrate for attachment (B. Berning, 2016, personal commun.). Grainstones consist almost exclusively of skeletal fragments of low-magnesium calcite (bryozoans, foraminifera, rhynchonellids) or magnesium calcite (red algae, echinoderms). Bioclasts that originally consisted of aragonite, such as calcareous green algae, bivalves, and gastropods, are very rare and only preserved as biomolds filled with later diagenetic products.

Diagenesis

Diagenetic sequences of the grainstones are quite uniform and subdivided into two types (Table 3B). Type A sequences mostly initiated with dissolution of aragonitic bioclasts (e.g., gastropods), followed by precipitation of an isopachous fringe of radial-fibrous cement, whereas remnant pore spaces, if present, are filled with blocky calcite spar (Fig. 11).

In type B sequences, dissolution of aragonitic bioclasts was followed by geopetal infilling of lime mudstone and/or micropeloidal grainstone into biomolds and interstitial pores. In addition, sediment grains are bound by micritic meniscus and/or pendant cements; together, these micritic cements typically occur in patches and roughly stratiform lenses (Fig. 12). The infilling of internal sediments was locally interrupted by dissolution,

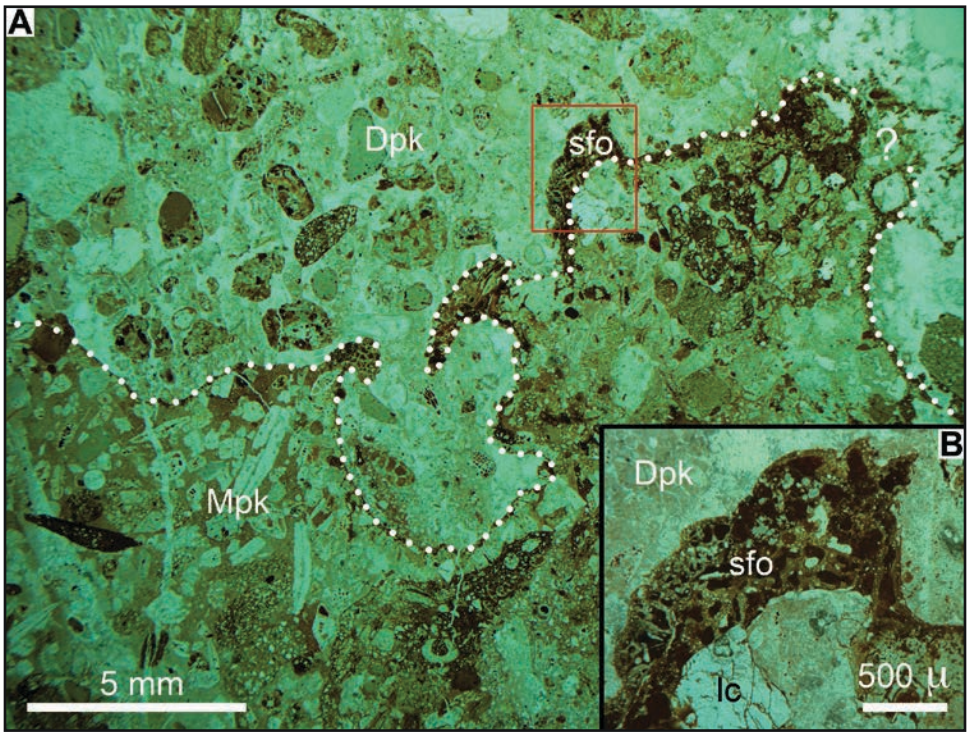

Figure 9. (A) K/P boundary hardground (white stipples) between Upper Maastrichtian larger foraminiferal packstone (Mpk) and Danian bio-lithoclastic packstone (Dpk). Note rugged hardground surface. Parallel nicols. Red rectangle shows sessile foraminifera (sfo). Parallel nicols. (B) Detail showing sessile foraminifera (sfo) on the hardground surface; lc—lithoclast in Maastrichtian limestone. Parallel nicols (µ—µm).

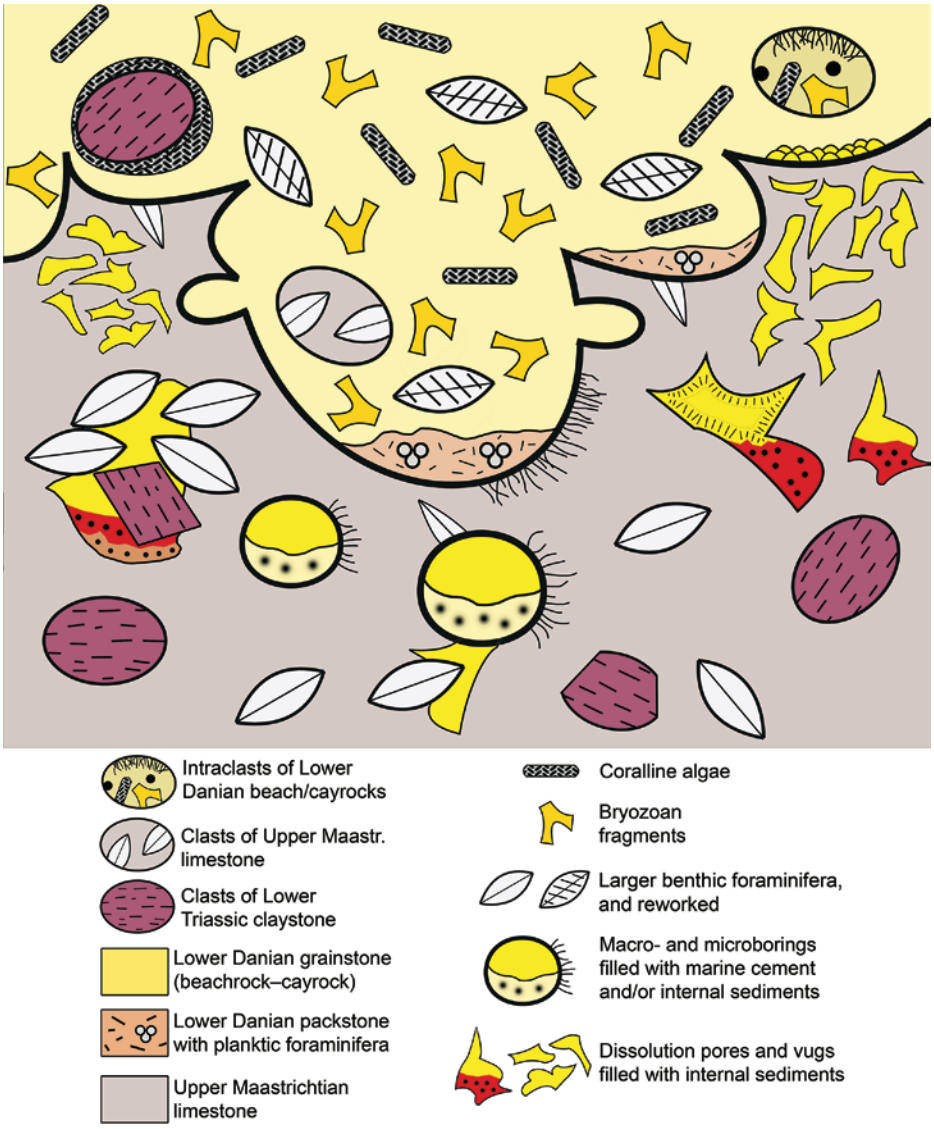

Figure 10. Graphic summary of K/P boundary hardground and associated phenomena.

resulting in micro-hardgrounds that vertically separate discrete phases of infill. The remaining pore space is filled with an isopachous fringe of radial-fibrous cement and/or blocky calcite spar (Fig. 12; Table 3B). Rock samples of primary packstone texture are rare. Sediment sorting in these packstones is identical to the more widespread grainstones. Packstones show dissolution vugs that may be entirely or partly filled with sediment and/or cements or micritic to micropeloidal sediment of probable bacterial origin.

Upper Danian

From the top of planktic foraminiferal zone P1a to the top of section 2, the nature of sedimentation remains constant and marked by well-sorted to poorly sorted bioclastic grainstones (rarely packstones) with fenestral pores, partly or entirely lithified by isopachous fringes of fibrous cement. In the upper part of the section, a hardground sharply separates a packstone from overlying packstones and grainstones (Fig. 13). The packstone beneath the hardground is intercalated into a succession of grainstones with fibrous cements and is riddled with multiple macroborings filled with reddish carbonate-lithic wackestone. Furthermore, the packstone is riddled with vugs filled with: (1) geopetal fabrics of lime mudstone to calcisiltite, and (2) a translucent cement with a crystal size too small to be clearly resolvable. The hardground is overlain by packstone and grainstone rich in intraclasts with packstone texture. Up section, only grainstone with fibrous cement was observed. Sampling of shorter outcrop exposures that are laterally correlative with larger outcrops indicated similar facies characteristics, at least for zones P1a to P1b (Fig. 6). These Danian sediments underlie bioclastic grainstones and packstones of ?Selandian to Thanetian age (Fig. 2) with similar facies and bioclast characteristics as the underlying Danian interval, except for the presence of larger fragments of corals and *Parachaetetes*.

TABLE 3. FEATURES OF LOWER DANIAN LIMESTONES

A: Sediment textures and components					
Texture, porosity		Main components		Taphonomy	
Grainstones strongly prevalent Pore types in grainstones: Fenestrae, shelter pores, biomolds after aragonitic components (e.g., gastropods), fissure pores, fractures filled with fibrous cement and/or internal sediments Rare: Poorly sorted packstones		Corallines, bryozoans, rhynchonellids, lithoclasts (older rocks), intraclasts, serpulids, echinoderm fragments, benthic foraminifera Lithoclasts disappear towards upper part of section		Sediment dominated by bioclasts of primary calcite (bryozoans, benthic foraminifera) and magnesian calcite (corallines) Many bio/intraclasts abraded, bored, encrusted, stained Bioclasts or biomolds indicative of primary aragonite are rare, in particular in the lower part of the section	
B: Diagenetic sequences. Key: R—rare; C—common; A—abundant.					
Type A sequence (left to right); typical of "beachrocks"					
R: Geopetal infilling of lime mud to micropeloidal grainstone in interstitial/intraskeletal pores before first cement precipitation	A: Dissolution of aragonite (biomoldic pores)		A: Fringes of radial-fibrous cement; this cement in many cases completely fills the intrinsic pore space		A: Blocky calcite spar in remnant pore space
Type B sequence (left to right); typical of "cayrocks"					
R: Geopetal infilling of lime mud to micropeloidal grainstone in interstitial/ intraskeletal pore space before start of diagenetic sequence	A: Dissolution of aragonite (biomoldic pores)	C: Geopetal infilling of lime mudstone to micropeloidal grainstone into (remnant) interstitial pore space and into biomolds	A: Micritic (meniscus) cement, micritic to microsparitic pendant cement; may overlap with preceding phase	C–A: Fringe of radial-fibrous cement; this cement may completely fill the remaining pore space	A: Blocky calcite spar in remnant pore space

DISCUSSION

Age and Depositional Environments

Age dating of the beachrock sequence across the K/P boundary transition at Kambühel is difficult because of its sparse and sporadic foraminiferal influx. Nevertheless, it was possible to estimate that the surface of the K/P boundary hardground represents a period of ~600 k.y. of nondeposition and erosion, which is similar to that of the deeper slope succession at Gamsbach in the eastern Alps (Punekar et al., 2016). The change from late Maastrichtian siliciclastic shelf deposition to terminal

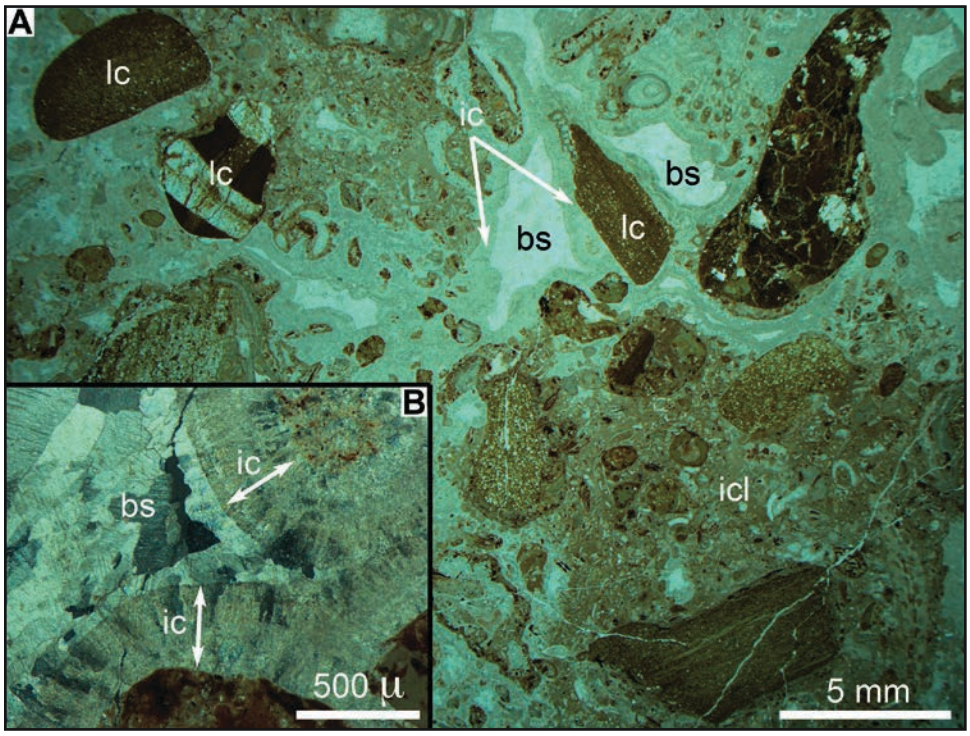

Figure 11. (A) Basal Danian bio-lithoclastic rudstone. Note (1) very poor sorting and sparse packing, and (2) lithoclasts of older rocks (lc, Werfen Formation) and intraclast of litho-bioclastic floatstone (icl). Most of the interstitial pore space is filled with an isopachous fringe of radial-fibrous cement (ic); remnant pore space is filled with blocky calcite spar (bs). Parallel nicols. (B) Detail of isopachous fringe of radial-fibrous cement (ic) showing typical sweeping extinction. Remnant pore space is filled with blocky calcite spar (bs). Crossed nicols (µ—µm).

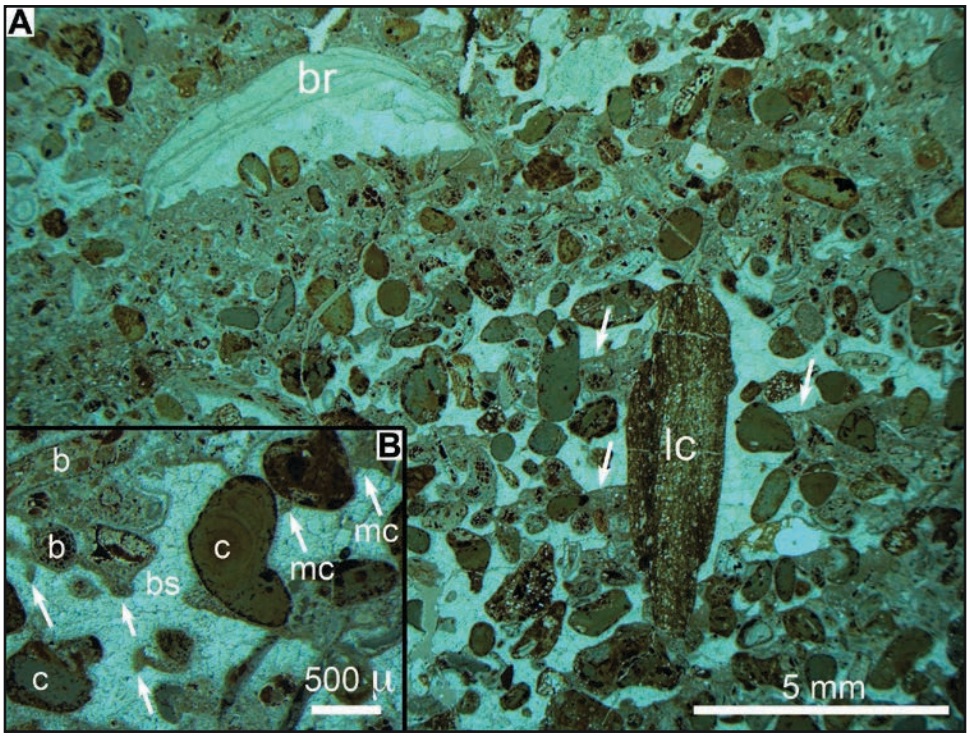

Figure 12. (A) Bio-lithoclastic grainstone of cayrock type. Stratification is evident by vertical change of levels with micritic cements (gray in photo) changing with indistinctly delimited levels rich in sparry cement. Note lithoclast (lc) and shelter pore under rhynchonellid shell (br). Note also interstitial geopetal infillings of lime mud (white arrows). Parallel nicols. (B) Detail of cayrock, showing microbored coralline algal fragments (c) and bryozoan fronds (b) with micritic pendant cements and meniscus cement (mc, marked by arrows); remnant pore space is filled with blocky calcite spar (bs). Parallel nicols (µ—µm).

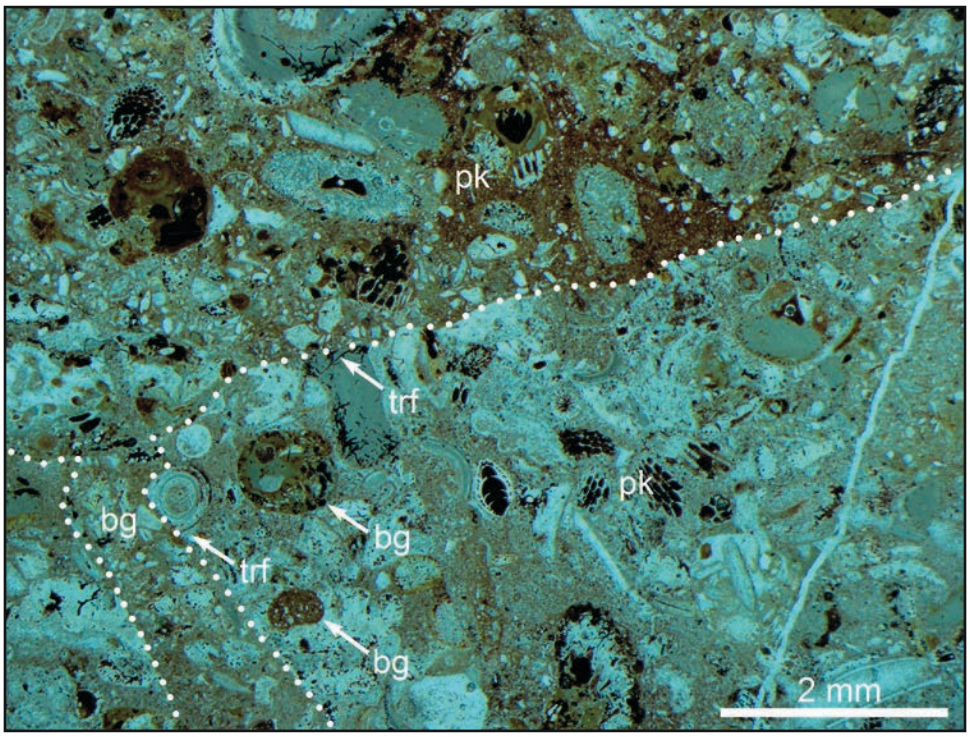

Figure 13. Hardground (stippled) within the Lower Danian succession (see Fig. 4 for position within section 2). White arrows show truncated fossils (trf); bg—borings; pk—packstone. Parallel nicols. The hardground is associated with a hiatus 1.5 m.y. in duration (see Fig. 6).

Maastrichtian–Paleocene shallow-water limestones (see Figs. 2 and 3) was not confined to beachrocks of the Kambühel area. In bathyal to abyssal successions deposited along the slope of the orogenic wedge, beds of carbonate-lithic turbidites and megaliths up to hundreds of meters in size record a Paleocene carbonate platform, which was cannibalized by synorogenic uplift and erosion (Tollmann, 1976; Wagreich and Faupl, 1994).

Biostratigraphic data indicate that platforms persisted during the Paleocene, but may have been localized (Tragelehn, 1996). Similarly, Eocene neritic limestones are rarely preserved in place (Van Hinte, 1963; Darga, 1990; Rasser, 1994), and most records are from clasts reworked into molasse deposits (e.g., Hagn, 1972, 1989; Moussavian, 1984; Rasser, 2000). Due to progressive Late Cretaceous to Paleogene onlap onto the accretionary wedge (Wagreich and Faupl, 1994), potential provenance areas for siliciclastics were overstepped, which favored the establishment of shallow-water platforms. This suggests that deposition of Paleocene to Eocene shallow-water limestones was widespread in the eastern Alps, but determining the precise extent is elusive (Nebelsick et al., 2005). The Paleogene resurgence of neritic carbonate deposition over large parts of the Alps was probably related mainly to tectonism rather than climatic aridification.

Maastrichtian and Danian Limestones

Bioperforations, infillings of diagenetic cavities, and diagenetic alterations of sediments yield important information about seafloor occupants, substrate conditions, and postdepositional overprint. In the Kambühel area, Maastrichtian limestones underlying Lower Danian limestones are marked by vugs and cavities with haloes of diagenetic grainstones. These cavities probably formed during subaerial exposure, whereas their multiphase infillings of red-colored mudstone and/or of grainstones resulted from the subsequent marine transgression. During subaerial exposure, the Kambühel area probably was a karstic terrain covered by soil. Upon transgression, the soil was stripped, and a rocky shore—the K/P boundary hardground—developed (Fig. 14). The complicated relief of the bored and encrusted hardground resulted from physico-chemical and biological processes in the shallow subtidal to supratidal zone of a low-energy rocky shore (cf., e.g., Trudgill, 1976; Laborel and Laborel-Deguen, 1996; Spencer and Viles, 2002; Twidale et al., 2005; Moura et al., 2006). Field mapping and biostratigraphy indicate that a steep relief of substrate rocks (e.g., buried cliffs or karst towers) is absent in the Kambühel area. Despite the potentially complex microscale morphology, this transgressive shore is reminiscent of a shore platform (cf. Moura et al., 2006).

The radial-fibrous cements in the Danian grainstones most probably precipitated from supersaturated seawater pumped through the pore space of sandy to fine-pebbly sediment. Absolute concentrations determined by EPMA yielded no conclusive information about the origin of the cement (see Methods section). We attribute this to repeated meteoric-diagenetic overprinting during episodes of subaerial exposure. Meteoric diagenesis is recorded by presence of cayrocks in the section and probably by the hardground identified in the Lower Danian succession. Overprint of fibrous cements, most probably by meteoric diagenetic processes, is underscored by their highly variable preservation even within single thin sections.

We saw no evidence that the radial-fibrous cements originated in a terrestrial setting far landward of the shoreline, or in a deep (few tens of meters) neritic setting. In the former case, a strong meteoric-vadose overprint of the grainstones would be expected, which contradicts the pervasive radial-fibrous isopachous cementation. In the latter case, intercalated intervals of deep neritic deposits (e.g., marls with planktonic foraminifera) would be expected. Isopachous radial-fibrous cements are typically of marine origin and result from percolation of seawater supersaturated with aragonite and (magnesian) calcite through the sediment pore space (e.g., Bathurst, 1975; Davies, 1977; Tucker and Wright, 1990; Tobin and Walker, 1996; James and Jones, 2016). Isopachous cement of fibrous aragonite may form even in meteoric-vadose settings, yet such cements are confined to patches a few centimeters wide (Ostermann et al., 2007). Notwithstanding the original polymorphy (or polymorphies) of cements, the pervasive isopachous radial-fibrous cementation is best interpreted as of shallow-marine origin.

Because of their initial lithification by isopachous radial-fibrous cements of shallow-marine origin, the grainstones represent beachrocks (cf., Bathurst, 1975; Flügel, 2004; Vousdoukas et al., 2007; Friedman, 2011). These may be subdivided into: (1) beachrocks *sensu stricto*, with marine-isopachous cement as the main first precipitate, and (2) cayrocks with micritic cements formed under vadose conditions as the major early diagenetic product (see, e.g., Bathurst, 1975; Gischler and Lomando, 1997; Friedman, 2011; Erginal et al., 2013; Christ et al., 2015). Because the entire Danian interval in section 2 (Fig. 4) consists mainly of beachrocks and cayrocks, this interval probably consists of stacked units separated by diastems and/or hiatuses (cf., e.g., Cooper, 1991; Vousdoukas et al., 2007; May et al., 2012; Erginal et al., 2013). A stacking of beachrock/cayrock layers requires net relative sea-level rise, albeit interrupted by nondeposition and erosion (Fig. 14). The abundant evidence for abrasion, bioerosion, and encrustation of bioclasts before final embedding records longer exposure on the seafloor at a low rate of sediment accumulation.

Skeletal Assemblages

Macrofossil and microfossil assemblages yield important information about the depositional environment, including nutrients, salinity, oxygen, and temperature. For example, an assemblage of bryozoans, red algae, and brachiopods may indicate cool-water and/or high-nutrient conditions (e.g., Carannante et al., 1988; James et al., 1992; Bone and James, 1993; Boreen et al., 1993; Vecsei and Sanders, 1999; Jaramillo-Vogel et al., 2016). In the Lower Danian limestones at Kambühel, bryozoans may reflect the cooling after the K/P boundary event that

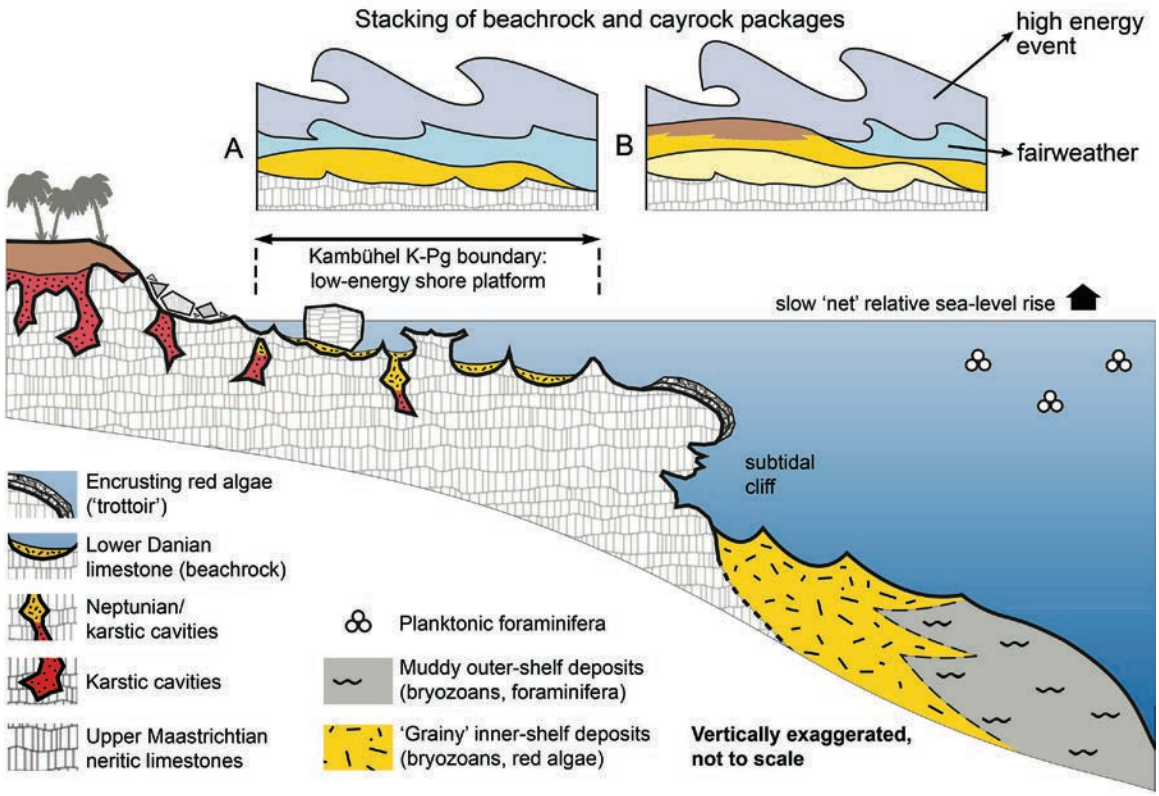

Figure 14. Hypothetical scenario to explain the Cretaceous-Paleogene (K-Pg) boundary hardground and the overlying Danian section. See text for description and discussion.

is known from stable isotopes of benthic foraminifera at Elles, Tunisia, and elsewhere (Stüben et al., 2003, 2005). Some workers attributed this cooling to the aftereffects of the Chicxulub impact (Galeotti et al., 2004; Vellekoop et al., 2015). However, the long-term nature of this cooling, concurrent delayed biological recovery and coincident with Deccan volcanism through the early Danian C29r and into C29n, strongly points to Deccan volcanism–related climate change (Keller et al., 2011a, this volume; Punekar et al., 2014). At Kambühel, the preserved Lower Danian sediments rich in bryozoans above the K/P boundary hardground were deposited in the upper zone P1a(1) (planktonic foraminifera) at least 150 k.y. after the K/P boundary event.

Articulate brachiopods flock on hard substrates, such as flanks and shady overhangs of cliffs or boulders. Intervals with abundant articulate brachiopods probably accumulated during storms (cf. Sedgwick and Davis, 2003; Marriner et al., 2017) and/or tsunamis (cf. Donato et al., 2008; Massari et al., 2009), which may have contributed to beachrock aggradation (cf., Morton et al., 2007; Wang and Horwitz, 2007). Similarly, coralline algae and bryozoans prefer hard-substrate habitats (cf., e.g., Betzler et al., 2000; James and Bone, 2011; James et al., 2013). Because beachrock formation steadily modifies the shore zone in favor of cemented substrate (Cooper, 1991; Vousdoukas et al., 2007), this may help to explain the persistence of hard-substrate biota in the Lower Danian section at Kambühel.

Extreme scarcity of colonial coral fragments in the Lower Danian section of the Kambühel limestone is probably unrelated to the mass extinction. Reef corals suffered only modest diversity loss across the K/P boundary transition (Kiessling and Baron-Szabo, 2004), and coral reefs grew again during the Danian (e.g., Vecsei and Moussavian, 1997; Vecsei et al., 1998; Baceta et al., 2005). In the Pyrenean Basin, shelf-edge coral reefs coexisted with foreslopes rich in bryozoans and red algal fragments (Baceta et al., 2005; Aguirre et al., 2007). At Kambühel, the common presence of the encrusting acervulinid foraminifer *Solenomeris* (Schlagintweit et al., 2018) suggests that the scarcity of corals may be explained by other factors. Comparative analysis of *Solenomeris* in Danian and Ypresian strata of the Pyrenees indicated that this species was resilient to siltation and lower illumination, which would adversely affect corals and coralline algae (Plaziat and Perrin, 1992). *Solenomeris* may have bloomed at Kambühel due to reduced competition with corals and corallines related to transgressive soil reworking and an overall higher resilience to unstable habitat conditions (Schlagintweit et al., 2018).

The depositional setting of the Gosau Group thus was composed of shelf sectors with coral reefs coexisting with rocky shores characterized by bryozoans, coralline algae, and brachiopods (for similar examples in the Miocene, see Moissette et al., 2007; Reuter et al., 2012). As mentioned, the total sedimentological evidence indicates that the Gosau shelves were relatively

narrow and steep. Such shelves are vulnerable to coastal upwelling. Thus, at least the shelf sectors fringed by rocky shores may have been episodically impinged by cooler, nutrient-rich waters. Together, the evidence suggests that the Lower Danian bryozoan–red algal–brachiopod assemblage of Kambühel was not related to coral extinction or to exceptional oceanographic conditions, but rather resulted from normal processes in the given depositional setting—a transgressive shore rich in hard substrates and associated biohabitats.

Global and Regional Perspectives of K/P Boundary Records

The Kambühel stratigraphic and hiatus records are complex, and viewed in isolation, they could be seen as simply local phenomena of little or no consequence to the overall history of sedimentation and depositional environments across the K/P boundary. However, when viewed within the global stratigraphic context of late Maastrichtian to Early Paleocene sedimentation and hiatus patterns, this shallow carbonate platform and rocky shore yield important information about the environmental effects at the continental margins. To elucidate this little-known environment during the K/P boundary transition, we briefly review and illustrate the global stratigraphy and erosional patterns of shelf to deep-marine environments. We then compare this record with Kambühel and other known marginal marine platform carbonates and siliciclastic sequences with the objective to place them within the larger historical context of the K/P boundary mass extinction event.

How Complete Is the K/P Boundary Transition in the Deep Sea?

The K/P boundary transition has been documented in over 300 sections worldwide, from continental shelf to deep-water environments that largely yield excellent stratigraphic records with high-resolution age control based on diverse and abundant planktonic foraminiferal and nannofossil assemblages (reviews in Keller, 2008, 2011b; Keller et al., 2013; Punekar et al., 2014; Thibault et al., 2016). The most complete K/P boundary records are known from shelf to upper-slope environments in Tunisia, particularly, the El Kef K/P boundary stratotype, although this section has a tectonically disturbed Maastrichtian section (Keller, 1988; Keller et al., 1996, 2002; Li and Keller, 1998a; Li et al., 2000; Keller et al., 2016a). In contrast, the auxiliary stratotype Elles section, located 75 km to the northeast and deposited on the continental shelf, has undisturbed sedimentation with high terrigenous influx (e.g., Abramovich and Keller, 2002; Keller et al., 1996, 2002; Molina et al., 2006; Thibault et al., 2016). Nonetheless, high-resolution quantitative faunal, stable isotopic, and cyclostratigraphic age controls reveal that even these two stratotype localities have short hiatuses in the early Danian, similar to localities in Egypt, Israel, and Spain (Punekar et al., 2014, 2016; Font et al., 2016, 2017). During the Maastrichtian, deep-sea hiatuses are relatively few and erosion is limited at the C31r/C31n and C30n/C29r transitions and within C30n (Fig. 15).

Deep-sea hiatuses generally correlate with climate cooling, sea-level falls, intensified oceanic circulation, and Deccan volcanism (Fig. 15), as supported by the fact that similar early Danian hiatuses are observed in marine sequences worldwide (Keller et al., 2016a, 2016b; Mateo et al., 2017). However, the extent of erosion is variable. In sequences with high sediment accumulation rates on continental shelves and upper slopes (e.g., Tunisia, Egypt, Israel, Spain), erosion is relatively limited. However, on topographic highs, such as mid-ocean ridges (e.g., Ninetyeast Ridge DSDP Sites 216, 217], Walvis Ridge [Site 525]), and uplifted areas of southern India (Cauvery Basin) and Madagascar (due to doming associated with Deccan volcanism), erosion is extensive in the early Danian and may encompass most or all of the early Danian and upper part of the Maastrichtian (see refs in Fig. 15). Additional localities with similar erosion patterns include the Caribbean Plateau (Sites 999B, 1001), North Atlantic Blake Nose (Sites 1049, 1050), and New Jersey (Bass River; Keller et al., 2013; Mateo et al., 2016, 2017).

How Complete Is the K/P Boundary Transition in Nearshore Settings?

Shallow-neritic K/P boundary sequences and associated biotic turnovers are relatively poorly documented, particularly in carbonate platform settings, which generally include major hiatuses spanning from several hundred thousand to millions of years (e.g., Guatemala, Belize, Oman, southern Mexico; Keller et al., 2003a, 2003b; Stinnesbeck et al., 1997; Ellwood et al., 2003, for Oman; see Fig. 16). Similarly, hiatuses are common in shallow nearshore areas or inland basins with high siliciclastic input, such as Argentina, Brazil, southern Tunisia, Denmark, and Texas (Fig. 16; Keller et al., 1997, 2007, 2011a, 2011b; Gertsch et al., 2013). The stratigraphic extent of these hiatuses is variable and in many cases uncertain due to low species diversity and rarity or absence of index microfossils.

In the western Tethys domain, shallow-water K/P boundary transitions are reported from the northern margin of the Apulian Platform (Vecsei et al., 1998), the Adriatic Platform (Drobne et al., 1996; Caffau et al., 1998; Korbar et al., 2015, 2017), and from locations in Turkey (Sirel, 1998, 2015; Inan and Inan, 2014). These carbonate platform sections represent shelfal to reefal environments and/or internal platform settings. In the Pyrenean Basin, absence of coral reefs during the early Danian is related to the depositional setting rather than the extinction of hermatypic corals, because coral reefs return during the later Danian (cf. Baceta et al., 2005; Aguirre et al., 2007).

In the eastern Alps, the Gamsbach valley section of Austria is a deep-water analog of the rocky shore Kambühel section. At this locality, the K/P boundary is documented from an upper-slope sequence (500–1000 m water depth) where the K/P boundary hiatus spans part of the latest Maastrichtian zone CF1, plus zone P0, part of zone P1a(1), and part of zone P1a(2) (Punekar et al., 2016), for an estimated total of ~500 k.y. (Fig. 16). This hiatus thus spans the mass extinction of all but the disaster opportunist *Guembelitria cretacea*, the sole long-term survivor. The top of

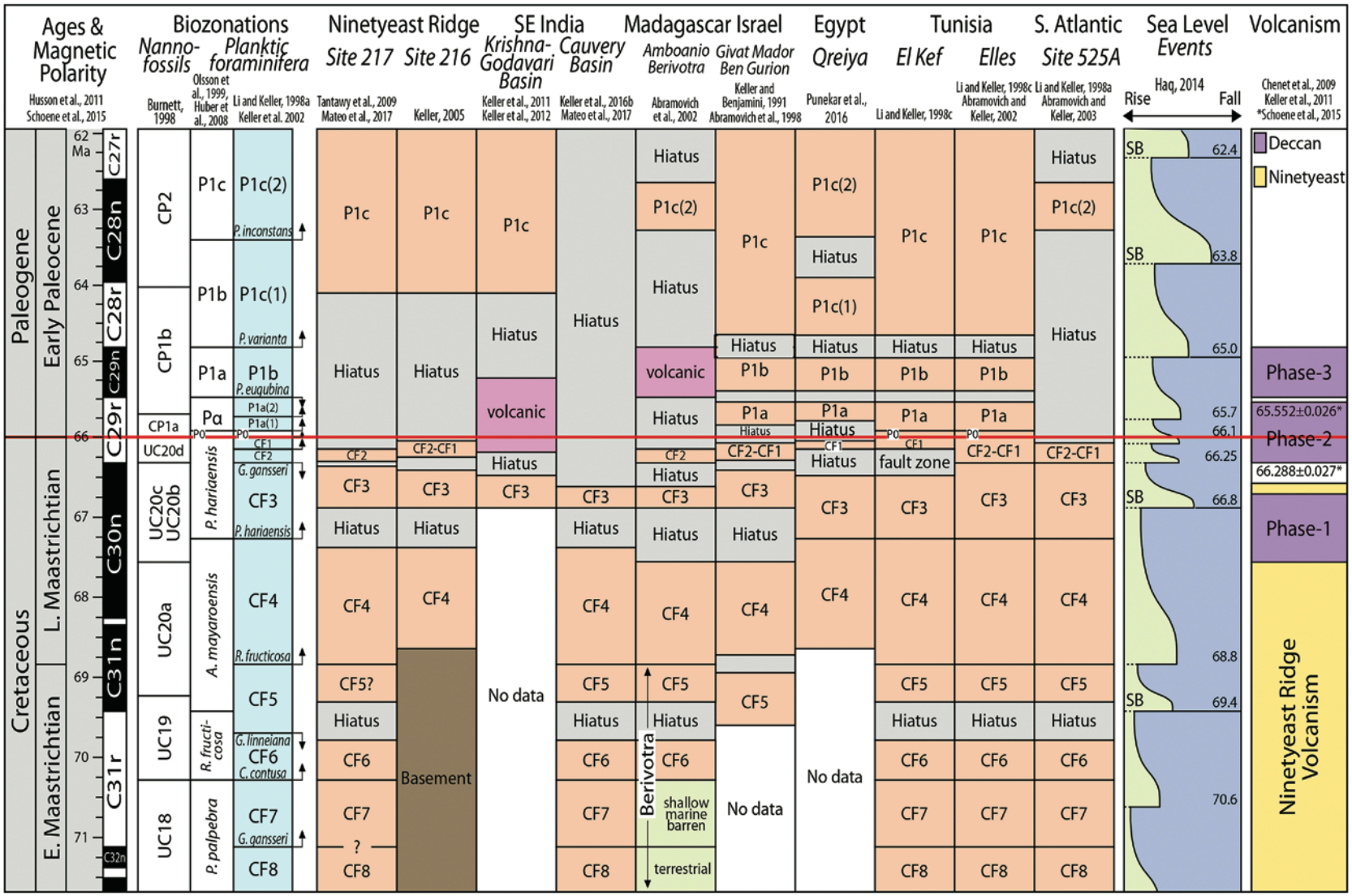

Figure 15. Sediment deposition and erosion (hiatus) events during the Maastrichtian–early Paleocene from the Indian Ocean to the Tethys and South Atlantic (Abramovich et al., 1998; Li and Keller, 1998a, 1998c; Keller and Benjamini, 1991; Abramovich et al., 2002; Abramovich and Keller, 2002; Keller, 2005; Tantawy et al., 2009; Keller et al., 2011a, 2012, 2016b; Punekar et al., 2014; Mateo et al., 2017) plotted against the magnetic polarity time scale of DSDP Site 525A (Husson et al., 2011), sea-level events (Haq, 2014), and Deccan and Ninetyeast Ridge volcanism (Chenet et al., 2009; Keller et al., 2011a, 2016a; Schoene et al., 2015). Biostratigraphy is based on planktic foraminifera and the zonation of scheme of Keller et al. (2002) and Li and Keller (1998a, 1998b); other zonal schemes are shown for comparison (Burnett, 1998; Olsson et al., 1999; Huber et al., 2008). Note the global distribution of hiatuses correlates with sea-level falls and major erosion on topographic highs (e.g., Ninetyeast Ridge, SE India, Walvis Ridge, South Atlantic) and the most complete sedimentary sequences (e.g., minor hiatuses) on continental shelves of Tunisia, Egypt, and Israel. Figure is modified from Mateo et al. (2017). E.—early; L.—late. SB—sequence boundary. CF—Cretaceous foraminifera. Key to foraminiferal genera: *Praemurica inconstans*, *Parasubbotina varianta*, *Parvularuglobigerina eugubina*, *Gansserina gansseri*, *Pseudoguembelina hariaensis*, *Abathomphalus mayaroensis*, *Racemiguembelina fructicosa*, *Globotruncana linneiana*, *Pseudoguembelina palpebra*, *Contusotruncana contusa*.

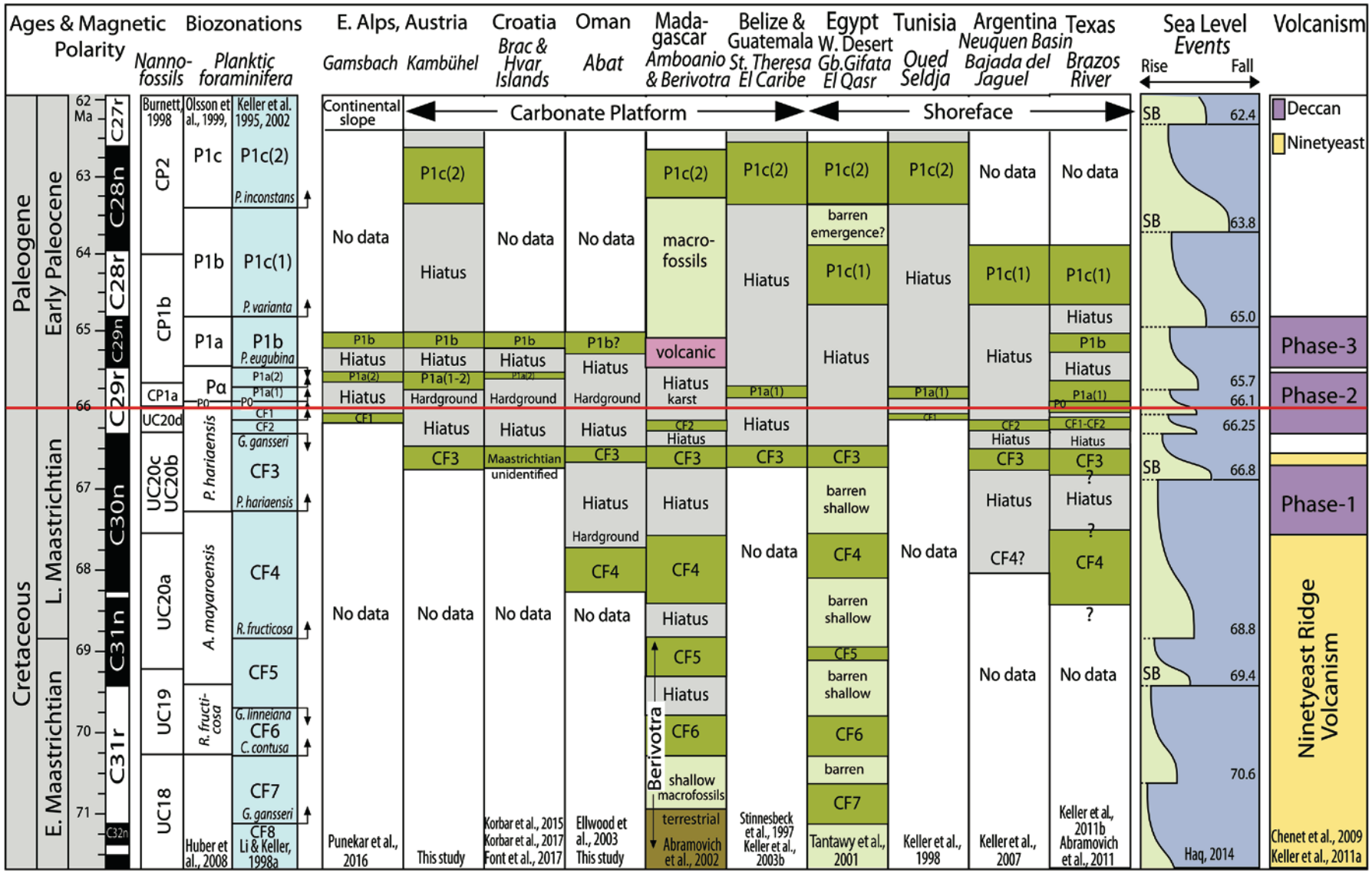

Figure 16. Sediment deposition and erosion (hiatus) events during the Maastrichtian–early Paleocene for carbonate platform and shoreface environments from the eastern Alps, eastern Tethys, and Indian Ocean to South Atlantic (Stinnesbeck et al., 1997; Keller et al., 1997; Tantawy et al., 2001; Ellwood et al., 2003; Abramovich et al., 2002, 2011; Keller, 2005; Keller et al., 2003b, 2007, 2011b; Punekar et al., 2016; Korbar et al., 2015, 2017; Font et al., 2017) plotted against the magnetic polarity time scale of DSDP Site 525A (Husson et al., 2011), sea-level events (Haq, 2014), and Deccan and Ninetyeast Ridge volcanism (Chenet et al., 2009; Keller et al., 2011a, 2012; Schoene et al., 2015). Biostratigraphy is based on planktic foraminifera and the zonation of scheme of Keller et al. (2002) and Li and Keller (1998a, 1998b); other zonal schemes are shown for comparison (Burnett, 1998; Olsson et al., 1999; Huber et al., 2008). Note that the global distribution of hiatuses in shallow platform and shoreface environments correlates with sea-level falls, similar to the deep-sea but generally with greater erosion and hardgrounds linked to subaerial emergence. See Figure 15 for key to abbreviations.

this hiatus is marked by the simultaneous appearances of 14 new early Danian species that are known to have evolved sequentially during the early Danian—zones P0, P1a(1), P1a(2). There is no K/P boundary clay (P0), which is confirmed by the abrupt shift in $\delta^{13}C$ values from Maastrichtian to early Danian (Grachev et al., 2005; Punekar et al., 2016).

Hiatus Distribution in Shallow Waters

Carbonate platform environments, such as Kambühel, are relatively common but rarely studied in depth and with good age control. For comparison with Kambühel, we chose similar environments from Croatia, Oman, Madagascar, Belize, and Guatemala (Fig. 16). Hiatuses were identified based on erosion surfaces, hardgrounds, and karstification. Age control was based on characteristic foraminifer biozone assemblages, which are frequently absent or only partly represented. From the emerging pattern of preserved partial biozones, it is clear that the hiatus distribution is very similar in all these geographically widespread areas, indicating a global imprint, even though the extent of erosion is variable (Fig. 16). Erosion was most extensive during the early Paleocene in the early part of magnetochrons C28n to late C29n, early Danian C29r to C29n, and late Maastrichtian C29r and C30n. The few records available for the early and late Maastrichtian also show correlative hiatuses. The most significant feature for the K/P boundary transition is the absence of the mass extinction interval in all carbonate platform sections, generally due to hardgrounds and/or karstification. In most cases, a partial record of the early Danian C29r is present (partial zones P1a[1] and/or P1a[2]) and a partial record of C29n is present (partial zone P1b]; Fig. 16). Thus, only a small part of the first ~400 k.y. of early Danian C29r (zones P0, P1a[1], P1a[2]) is present in any shallow carbonate platform environment. Moreover, erosion and/or nondeposition spans C29r below the K/P boundary and into C30n (CF1-CF2) for ~500 k.y. Only rarely is this interval partially present (e.g., Madagascar).

We also compared platform carbonates with shoreface siliciclastic deposition of inland seas with high terrigenous inputs, such as in Egypt, Tunisia, Argentina, and Texas (Fig. 16). Except for Texas (Brazos River), the K/P boundary is also absent in these environments, and early Danian erosion removed also the latest Maastrichtian record. This may have been due to lower terrigenous input, sea-level fluctuations, seasonal storms, and/or regional uplift, which may have acted in concert to amplify erosion of underlying sediments.

A rare exception is the Brazos River paleoenvironment of Texas, where a dozen outcrops and cores reveal a shallow nearshore environment marked by local topographic highs and associated variable erosion patterns. This environment at the shore of the Western Interior Seaway was tectonically stable with high terrigenous influx and boasts the most complete shallow-water sequence known to date (Adatte et al., 2011). The Brazos River environment shallowed from middle neritic depth during the late Maastrichtian zone CF2 to inner neritic depth with a sharp sea-level drop in CF1. In the deeper inner neritic parts, the sea-level fall was accompanied by erosion, which carved submarine channels that infilled with shore debris, shell hash, glauconite, and Chicxulub impact spherules (Keller et al., 2011b). Normal deposition continued above these channel deposits and preserved the K/P boundary transition as well as most of the early Danian zones P0 and P1a(1), followed by another hiatus between P1a(1) and P1b (Fig. 16). However, on local topographic highs (Darting Minnow Creek), only the channel deposit is present, followed by zone P1a(2). In a core drilled just 150 m from Darting Minnow Creek, an unconformity marks a mangrove root level in zone CF1, channel deposits are absent, and sedimentation resumed in zone P1a(2) (Fig. 16; Adatte et al., 2011).

Brazos River sections thus reveal the different expressions of sea-level change and resulting patterns of sediment dispersal and erosion in relation to variable topography. Nevertheless, the hiatus distributions of neritic environments generally reveal the same pattern as in deep-water environments. We conclude that despite very different depositional settings in platform carbonates, shoreface siliciclastic, and deep marine environments, hiatus patterns indicate the same underlying causes at work (e.g., sea-level fall, subaerial to submarine erosion, climate cooling) in shallow- and deep-sea environments, even though erosion is generally more extensive in shallow-water settings (Figs. 15 and 16).

CONCLUSIONS

(1) In a synorogenic succession of Upper Maastrichtian to Thanetian shallow-water limestones (Kambühel Formation) of the eastern Alps, the K/P boundary is marked by a hardground and a hiatus that juxtaposes late Maastrichtian zone CF3 (*Pseudoguembelina hariaensis*) and early Danian (upper P1a[1] zone), indicating an ~600 k.y. gap due to nondeposition and erosion.

(2) The Upper Maastrichtian part of the succession consists of bioturbated packstones rich in larger benthic foraminifera (e.g., *Orbitoides*, *Lepidorbitoides*, *Siderolites*, *Clypeorbis*) and planktic foraminifera (e.g., *Pseudoguembelina*, *Planoglobulina*). These limestones are riddled with (micro)karstic cavities near their top, and, particularly along the margins of dikes, they are transformed by dissolution of interstitial matrix into diagenetic grainstones. Dikes are filled with Lower Danian bio-lithoclastic grainstones to rudstones rich in fragments of coralline algae, bryozoans, and clasts derived from Maastrichtian limestones and Triassic rocks.

(3) The K/P boundary hardground reveals a bizarrely cusped relief upon Maastrichtian limestones penetrated by borings and/or encrusted by sessile organisms (e.g., foraminifera, serpulids). Overlying Lower Danian deposits are poorly sorted bio-lithoclastic grainstones with fenestral pores and isopachous fringes of radial-fibrous cement. Deposition during the early Danian transgression occurred on a rocky low-energy shore that experienced episodic high-energy events.

(4) Another hardground in the Upper Danian is overlain by beachrocks and cayrocks characterized by fragments of bryozoans (cheilostomes, cyclostomes), red algae, lithoclasts from older rocks, and intraclasts. The presence of planktic foraminiferal assemblages indicates a period of nondeposition and erosion that brackets a hiatus of ~1.5 m.y. Deposition occurred in persistent hard-substrate conditions on a rocky shelf, as indicated by the bryozoan–coralline algal composition of the beachrocks–cayrocks.

(5) In the Upper Thanetian, floatstones to bafflestones with colonial corals, solenoporaceans (*Parachaetetes*), foliose corallines, milioline foraminifera, and dasycladalean algae record the establishment of an open, shallow subtidal habitat with lime-muddy substrate.

(6) We compared the Kambühel shallow-water K/P boundary transition with similar shallow-water transitions globally and with the global deep-sea record. The comparison reveals very similar patterns in shallow- and deep-water environments, although erosion is more extensive and sequences are less complete in shallow waters due to sea-level falls and potential local tectonic activity. We conclude that climate and sea-level changes were the driving forces for the observed sedimentation and erosion patterns and that climate change across the K/P boundary transition (C29r-C29n) was mainly driven by Deccan volcanism.

ACKNOWLEDGMENTS

Financial support from grant "Nachwuchsförderung der Universität Innsbruck," project W715505 (to M. Studeny), is gratefully acknowledged. Martina Tribus, Institute of Mineralogy and Petrography, is thanked for her help and expertise in electron probe microanalytical measurements as well as in element mapping. Björn Berning, Biologiezentrum-Oberösterreichisches Landesmuseum Linz (Austria), is thanked for taxonomic affiliation of bryozoans in thin sections. The constructive comments by an anonymous reviewer and by Annie Arnaud-Vanneau improved the clarity of presentation. The University of Innsbruck is thanked for donating financial support for Gold Open Access publication.

REFERENCES CITED

Abramovich, S., and Keller, G., 2002, High stress late Maastrichtian palaeoenvironment in Tunisia: Inference from planktic foraminifera: Palaeogeography, Palaeoclimatology, Palaeoecology, v. 178, p. 145–164, https://doi.org/10.1016/S0031-0182(01)00394-7.

Abramovich S., and Keller, G., 2003, Planktonic foraminiferal response to the latest Maastrichtian abrupt warm event: A case study from South Atlantic DSDP Site 525A: Marine Micropaleontology, v. 48, p. 225–249, https://doi.org/10.1016/S0377-8398(03)00021-5.

Abramovich, S., Almogi-Labin, A., and Benjamini, C., 1998, Decline of the Maastrichtian pelagic ecosystem based on planktic foraminifera assemblage changes: Implication for the terminal Cretaceous faunal crisis: Geology, v. 26, p. 63–66, https://doi.org/10.1130/0091-7613(1998)026<0063:DOTMPE>2.3.CO;2.

Abramovich, S., Keller, G., Adatte, T., Stinnesbeck, W., Hottinger, L., Stueben, D., Berner, Z., Ramanivosoa, B., and Randriamanantenasoa, A., 2002, Age and paleoenvironment of the Maastrichtian-Paleocene of the Mahajanga Basin, Madagascar: A multidisciplinary approach: Marine Micropaleontology, v. 47, p. 17–70, https://doi.org/10.1016/S0377-8398(02)00094-4.

Abramovich, S., Keller, G., Berner, Z., Cymbalista, M., and Rak, C., 2011, Maastrichtian planktic foraminiferal biostratigraphy and paleoenvironment of Brazos River, Falls County, Texas, *in* Keller, G., and Adatte, T., eds., End-Cretaceous Mass Extinction and the Chicxulub Impact in Texas: Society of Sedimentary Geology (SEPM) Special Publication 100, p. 123–156.

Adatte, T., Keller, G., and Baum, G., 2011, Lithostratigraphy, sedimentology, sequence stratigraphy and the origin of the sandstone complex in the Brazos River KT sequences, *in* Keller, G., and Adatte, T., eds., End-Cretaceous Mass Extinction and the Chicxulub Impact in Texas: Society of Sedimentary Geology (SEPM) Special Publication 100, p. 43–80.

Aguirre, J., Baceta, J.I., and Braga, J.C., 2007, Recovery of marine primary producers after the Cretaceous-Tertiary mass extinction: Paleocene calcareous red algae from the Iberian Peninsula: Palaeogeography, Palaeoclimatology, Palaeoecology, v. 249, p. 393–411, https://doi.org/10.1016/j.palaeo.2007.02.009.

Baceta, J.I., Pujalte, V., and Bernaola, G., 2005, Paleocene coralgal reefs of the western Pyrenean basin, northern Spain: New evidence supporting an earliest Paleogene recovery of reefal ecosystems: Palaeogeography, Palaeoclimatology, Palaeoecology, v. 224, p. 117–143, https://doi.org/10.1016/j.palaeo.2005.03.033.

Bathurst, R.C., 1975, Carbonate Sediments and Their Diagenesis: Amsterdam, Elsevier, Developments in Sedimentology 12, 658 p.

Berggren, W.A., and Pearson, P.N., 2005, A revised tropical to subtropical Paleogene planktonic foraminiferal zonation: Journal of Foraminiferal Research, v. 35, p. 279–298, https://doi.org/10.2113/35.4.279.

Betzler, C., Martín, J.M., and Braga, J.C., 2000, Non-tropical carbonates related to rocky submarine cliffs (Miocene, Almería, southern Spain): Sedimentary Geology, v. 131, p. 51–65, https://doi.org/10.1016/S0037-0738(99)00125-6.

Bone, Y., and James, N.P., 1993, Bryozoans as carbonate sediment producers on the cool-water Lacepede Shelf, southern Australia: Sedimentary Geology, v. 86, p. 247–271, https://doi.org/10.1016/0037-0738(93)90025-Z.

Boreen, T., James, N.P., Wilson, C., and Heggie, D., 1993, Surficial cool-water carbonate sediments on the Otway continental margin, southeastern Australia: Marine Geology, v. 112, p. 35–56, https://doi.org/10.1016/0025-3227(93)90160-W.

Burnett, J., 1998, Upper Cretaceous, *in* Bown, P.R., ed., Calcareous Nannofossil Biostratigraphy: Cambridge, UK, Chapman and Hall, p. 132–199, https://doi.org/10.1007/978-94-011-4902-0_6.

Caffau, M., Plenicar, M., Pugliese, N., and Drobne, K., 1998, Late Maastrichtian rudists and microfossils in the Karst region (NE Italy and Slovenia): Geobios, v. 31, p. 37–46, https://doi.org/10.1016/S0016-6995(98)80063-6.

Carannante, G., Esteban, M., Milliman, J.D., and Simone, L., 1988, Carbonate lithofacies as paleolatitude indicators: Problems and limitations: Sedimentary Geology, v. 60, p. 333–346, https://doi.org/10.1016/0037-0738(88)90128-5.

Chenet, A.-L., Courtillot, V., Fluteau, F., Gerard, M., Quidelleur, X., Khadri, S.F.R., Subbarao, K.V., and Thordarson, T., 2009, Determination of rapid Deccan eruptions across the Cretaceous-Tertiary boundary using paleomagnetic secular variation: 2. Constraints from analysis of eight new sections and synthesis for a 3500-m-thick composite section: Journal of Geophysical Research–Solid Earth, v. 114, no. B6, B06103, https://doi.org/10.1029/2008JB005644.

Christ, N., Immenhauser, A., Wood, R.A., Darwich, K., and Niedermayr, A., 2015, Petrography and environmental controls on the formation of Phanerozoic marine carbonate hardgrounds: Earth-Science Reviews, v. 151, p. 176–226, https://doi.org/10.1016/j.earscirev.2015.10.002.

Clyde, W.C., Ramezani, J., Johnson, K.R., Bowring, S.A., and Jones, M.M., 2016, Direct high-precision U-Pb geochronology of the end-Cretaceous mass extinction and calibration of Paleocene astronomical cycles: Earth and Planetary Science Letters, v. 452, p. 272–280, https://doi.org/10.1016/j.epsl.2016.07.041.

Cooper, J.A.G., 1991, Beachrock formation in low latitudes: Implications for coastal evolutionary models: Marine Geology, v. 98, p. 145–154, https://doi.org/10.1016/0025-3227(91)90042-3.

Darga, R., 1990, The Eisenrichterstein near Hallthurm, Bavaria: An Upper Eocene carbonate ramp (Northern Calcareous Alps): Facies, v. 23, p. 17–33, https://doi.org/10.1007/BF02536705.

Davies, G.R., 1977, Former magnesian calcite and aragonite submarine cements in Upper Paleozoic reefs of the Canadian Arctic: A summary: Geology, v. 5, p. 11–15, https://doi.org/10.1130/0091-7613(1977)5<11:FMCAAS>2.0.CO;2.

Donato, S.V., Reinhardt, E.G., Boyce, J.I., Rothaus, R., and Vosmer, T., 2008, Identifying tsunami deposits using bivalve shell taphonomy: Geology, v. 36, p. 199–202, https://doi.org/10.1130/G24554A.1.

Drobne, K., Ogorelec, B., Dolenec, T., Marton, E., and Palinkaš, L., 1996, Biota and abiota at the K/T boundary in the Dolenja Vas sections, Slovenia, *in* Drobne, K., Goričan, Š., and Kotnik, B., eds., The Role of Impact Processes in the Geological and Biological Evolution of Planet Earth: International Workshop Postojna 1996: Ljubljana, n.p., p. 163–181.

Dulai, A., Bitner, M.A., and Müller, P., 2008, A monospecific assemblage of a new rhynchonellid brachiopod from the Paleocene of Austria: Fossils and Strata, v. 54, p. 193–201.

Ellwood, B.B., MacDonald, W.D., Wheeler, C., and Benoist, L.S., 2003, The K-T boundary in Oman: Identified using magnetic susceptibility field measurements with geochemical confirmation: Earth and Planetary Science Letters, v. 206, p. 529–540, https://doi.org/10.1016/S0012-821X(02)01124-X.

Erginal, A.E., Ekinci, Y.L., Demirci, A., Bozcu, M., Ozturk, M.Z., Avcioglu, M., and Oztura, E., 2013, First record of beachrock on Black Sea coast of Turkey: Implications for late Holocene sea-level fluctuations: Sedimentary Geology, v. 294, p. 294–302, https://doi.org/10.1016/j.sedgeo.2013.06.003.

Flügel, E., 2004, Microfacies of Carbonate Rocks: Berlin, Springer, 976 p., https://doi.org/10.1007/978-3-662-08726-8.

Font, E., Adatte, T., Keller, G., Abrajevitch, A., Sial, A.N., de Lacerda, D.L., and Punekar, P., 2016, Mercury anomaly, Deccan volcanism and the end-Cretaceous mass extinction: (Reply to Smit et al. 2016): Geology, v. 44, no. 3, p. e382, https://doi.org/10.1130/G37451.1.

Font, E., Keller, G., Sanders, D., and Adatte, T., 2017, Comment on "Post-impact event bed (tsunamite) at the Cretaceous-Paleogene boundary deposited on a distal carbonate platform interior": Terra Nova, v. 29, p. 329–331, https://doi.org/10.1111/ter.12282.

Friedman, G., 2011, Beachrocks record Holocene events, including natural disasters: Carbonates and Evaporites, v. 26, p. 97–109, https://doi.org/10.1007/s13146-011-0056-3.

Galeotti, S., Brinkhuis, H., and Huber, M., 2004, Records of post–Cretaceous-Tertiary boundary millennial-scale cooling from the western Tethys: A smoking gun for the impact-winter hypothesis?: Geology, v. 32, p. 529–532, https://doi.org/10.1130/G20439.1.

Gertsch, B., Keller, G., Adatte, T., and Berner, Z., 2013, The Cretaceous-Tertiary boundary (KTB) transition in NE Brazil: Journal of the Geological Society, v. 170, p. 249–262, https://doi.org/10.1144/jgs2012-029.

Gischler, E., and Lomando, A.J., 1997, Holocene cemented beach deposits in Belize: Sedimentary Geology, v. 110, p. 277–297, https://doi.org/10.1016/S0037-0738(96)00088-7.

Grachev, A.F., Korchagin, O.A., Kollmann, H.A., Pechersky, D.M., and Tsel'movich, V.A., 2005, A new look at the nature of the transitional layer at the K/T boundary near Gams, eastern Alps, Austria, and the problem of the mass extinction of the biota: Russian Journal of Earth Sciences, v. 7, ES6001, https://doi.org/10.2205/2005ES000189.

Hagn, H., 1972, Über kalkalpine paleozäne und untereozäne Gerölle aus dem bayerischen Alpenvorland: Mitteilungen der Bayerischen Staatssammlung für Paläontologie und Historische Geologie, v. 12, p. 113–124.

Hagn, H., 1989, Über einige bedeutsame Kreide- und Alttertiärgerölle aus der Faltenmolasse des Allgäus: Geologica Bavarica, v. 94, p. 5–47.

Håkansson, E., and Thomsen, E., 1999, Benthic extinction and recovery patterns at the K/T boundary in shallow water carbonates, Denmark: Palaeogeography, Palaeoclimatology, Palaeoecology, v. 154, p. 67–85, https://doi.org/10.1016/S0031-0182(99)00087-5.

Haldar, S.K., and Tisljar, J., 2014, Introduction to Mineralogy and Petrology: Amsterdam, Elsevier, 354 p.

Handy, M.R., Ustaszewski, K., and Kissling, E., 2015, Reconstructing the Alps-Carpathians-Dinarides as a key to understanding switches in subduction polarity, slab gaps and surface motion: International Journal of Earth Sciences, v. 104, p. 1–26, https://doi.org/10.1007/s00531-014-1060-3.

Haq, B.U., 2014, Cretaceous eustasy revisited: Global and Planetary Change, v. 113, p. 44–58, https://doi.org/10.1016/j.gloplacha.2013.12.007.

Huber, B.T., MacLeod, K.G., and Tur, N.A., 2008, Chronostratigraphic framework for Upper Campanian–Maastrichtian sediments on the Blake Nose (subtropical North Atlantic): Journal of Foraminiferal Research, v. 38, p. 162–182, https://doi.org/10.2113/gsjfr.38.2.162.

Husson, D., Galbrun, B., Laskar, J., Hinnov, L.A., Thibault, N., Gardin, S., and Locklair, R.E., 2011, Astronomical calibration of the Maastrichtian (Late Cretaceous): Earth and Planetary Science Letters, v. 305, p. 328–340, https://doi.org/10.1016/j.epsl.2011.03.008.

Inan, N., and Inan, S., 2014, Stratigraphic ranges of the benthic foraminifera and microfacies of the Upper Maastrichtian–Paleocene shallow marine carbonate successions in the Eastern Pontides (NE Turkey): Bulletin for Earth Sciences (Yerbilimleri), v. 35, p. 79–86.

James, N.P., and Bone, Y., 2011, Carbonate production and deposition in a warm-temperate macroalgal environment, Investigator Strait, South Australia: Sedimentary Geology, v. 240, p. 41–53, https://doi.org/10.1016/j.sedgeo.2011.07.005.

James, N.P., and Jones, B., 2016, Origin of Carbonate Sedimentary Rocks: Chichester, UK, John Wiley & Sons Ltd., 446 p.

James, N.P., Bone, Y., von der Borch, C.C., and Gostin, V.A., 1992, Modern carbonate and terrigenous clastic sediments on a cool-water, high-energy, mid-latitude shelf; Lacepede Shelf, southern Australia: Sedimentology, v. 39, p. 877–903, https://doi.org/10.1111/j.1365-3091.1992.tb02158.x.

James, N.P., Reid, C.M., Bone, Y., Levings, A., and Malcolm, I., 2013, The macroalgal carbonate factory at a cool-to-warm temperate marine transition, southern Australia: Sedimentary Geology, v. 291, p. 1–26, https://doi.org/10.1016/j.sedgeo.2013.03.007.

Jaramillo-Vogel, D., Bover-Arnal, T., and Strasser, A., 2016, Bryozoan beds in northern Italy as a shallow-water expression of environmental changes during the Oligocene isotope event 1: Sedimentary Geology, v. 331, p. 148–161, https://doi.org/10.1016/j.sedgeo.2015.10.006.

Johnson, C.C., Sanders, D., Kauffman, E.G., and Hay, W.W., 2002, Upper Cretaceous reefal patterns and processes affecting their development and demise, *in* Kiessling, W., Flügel, E., and Golonka, J., eds., Phanerozoic Reef Patterns: Society of Sedimentary Geology (SEPM) Special Publication 72, p. 549–585, https://doi.org/10.2110/pec.02.72.0549.

Keller, G., 1988, Extinction, Survivorship and Evolution across the Cretaceous/Tertiary Boundary at El Kef, Tunisia: Marine Micropaleontology, v. 13, p. 239–263, https://doi.org/10.1016/0377-8398(88)90005-9.

Keller, G., 2005, Biotic effects of late Maastrichtian mantle plume volcanism: Implications for impacts and mass extinctions: Lithos, v. 79, p. 317–341, https://doi.org/10.1016/j.lithos.2004.09.005.

Keller, G., 2008, Impact stratigraphy: Old principle, new reality, *in* Evans, K.R., Horton, J.W., and King, D.T., eds., The Sedimentary Record of Meteorite Impacts: Geological Society of America Special Paper 437, p. 147–178, https://doi.org/10.1130/2008.2437(09).

Keller, G., 2011a, Defining the K-T boundary: A practical guide and return to first principles, *in* Keller, G., and Adatte, T., eds., End-Cretaceous Mass Extinction and the Chicxulub Impact in Texas: Society of Sedimentary Geology (SEPM) Special Publication 100, p. 23–42.

Keller, G., 2011b, Cretaceous-Tertiary mass extinction in marginal and open marine environments in Texas, USA, and Tunisia, *in* Keller, G., and Adatte, T., eds., End-Cretaceous Mass Extinction and the Chicxulub Impact in Texas: Society of Sedimentary Geology (SEPM) Special Publication 100, p. 197–226.

Keller, G., 2014, Deccan volcanism, the Chicxulub impact, and the end-Cretaceous mass extinction: Coincidence? Cause and effect?, *in* Keller, G., and Kerr, A.C., eds., Volcanism, Impacts, and Mass Extinctions: Causes and Effects: Geological Society of America Special Paper 505, p. 29–55, https://doi.org/10.1130/2014.2505(03).

Keller, G., and Benjamini, C., 1991, Paleoenvironment of the eastern Tethys in the early Danian: Palaios, v. 6, p. 439–464, https://doi.org/10.2307/3514984.

Keller, G., Li, L., and MacLeod, N., 1996, The Cretaceous/Tertiary boundary stratotype section at El Kef, Tunisia: How catastrophic was the mass extinction?: Palaeogeography, Palaeoclimatology, Palaeoecology, v. 119, p. 221–254, https://doi.org/10.1016/0031-0182(95)00009-7.

Keller, G., Adatte, T., Stinnesbeck, W., Stuben, D., Kramar, U., Berner, Z., Li, L., and von Salis Perch-Nielsen, K., 1997, The Cretaceous-Tertiary transition on the shallow Saharan Platform in southern Tunisia: Geobios, v. 30, p. 951–975, https://doi.org/10.1016/S0016-6995(97)80218-5.

Keller, G., Adatte, T., Stinnesbeck, W., Stuben, D., Kramar, U., Berner, Z., Li, L., and von Salis Perch-Nielsen, K., 1998, The Cretaceous-Tertiary

ransition on the shallow Saharan Platform of southern Tunisia. Geobios, v. 30, p. 951–975. https://doi.org/10.1016/S0016-6995(97)80218-5.

Keller, G., Adatte, T., Stinnesbeck, W., Luciani, V., Karoui, N., and Zaghbib-Turki, D., 2002, Paleoecology of the Cretaceous-Tertiary mass extinction in planktic foraminifera: Palaeogeography, Palaeoclimatology, Palaeoecology, v. 178, p. 257–297, https://doi.org/10.1016/S0031-0182(01)00399-6.

Keller, G., Stinnesbeck, W., Adatte, T., and Stueben, D., 2003a, Multiple impacts across the Cretaceous-Tertiary boundary: Earth-Science Reviews, v. 62, p. 327–363, https://doi.org/10.1016/S0012-8252(02)00162-9.

Keller, G., Stinnesbeck, W., Adatte, T., Holland, B., Stueben, D., Harting, M., de Leon, C., and de la Cruz, J., 2003b, Spherule deposits in Cretaceous-Tertiary boundary sediments in Belize and Guatemala: Journal of the Geological Society, v. 160, p. 783–795, https://doi.org/10.1144/0016-764902-119.

Keller, G., Adatte, T., Tantawy, A.A., Berner, Z., and Stueben, D., 2007, High stress Late Cretaceous to early Danian paleoenvironment in the Neuquen Basin, Argentina: Cretaceous Research, v. 28, p. 939–960, https://doi.org/10.1016/j.cretres.2007.01.006.

Keller, G., Bhowmick, P.K., Upadhyay, H., Dave, A., Reddy, A.N., Jaiprakash, B.C., and Adatte, T., 2011a, Deccan volcanism linked to the Cretaceous-Tertiary boundary (KTB) mass extinction: New evidence from ONGC wells in the Krishna-Godavari Basin, India: Journal of the Geological Society of India, v. 78, p. 399–428, https://doi.org/10.1007/s12594-011-0107-3.

Keller, G., Abramovich, S., Adatte, T., and Berner, Z., 2011b, Biostratigraphy, age of the Chicxulub impact and depositional environment of the Brazos River KT sequences, *in* Keller, G., and Adatte, T., eds., End-Cretaceous Mass Extinction and the Chicxulub Impact in Texas: Society of Sedimentary Geology (SEPM) Special Publication 100, p. 81–122.

Keller, G., Adatte, T., Bhowmick, P.K., Upadhyay, H., Dave, A., Reddy, A.N., and Jaiprakash, B.C., 2012, Nature and timing of extinctions in Cretaceous-Tertiary planktic foraminifera preserved in Deccan intertrappean sediments of the Krishna-Godavari Basin, India: Earth and Planetary Science Letters, v. 341–344, p. 211–221, https://doi.org/10.1016/j.epsl.2012.06.021.

Keller, G., Malarkodi, N., Khozeym, H., Adatte, T., Spangenberg, J.E., and Stinnesbeck, W., 2013, Chicxulub impact spherules in the NW Atlantic and Caribbean: Age constraints and KTB hiatus: Geological Magazine, v. 150, p. 885–907, https://doi.org/10.1017/S0016756812001069.

Keller, G., Punekar, J., and Mateo, P., 2016a, Upheavals during the late Maastrichtian: Volcanism, climate and faunal events preceding the end-Cretaceous mass extinction: Palaeogeography, Palaeoclimatology, Palaeoecology, v. 441, p. 137–151, https://doi.org/10.1016/j.palaeo.2015.06.034.

Keller, G., Jaiprakash, B.C., and Reddy, A.N., 2016b, Maastrichtian to Eocene subsurface stratigraphy of the Cauvery Basin and correlation with Madagascar: Journal of the Geological Society of India, v. 87, p. 5–34, https://doi.org/10.1007/s12594-016-0370-4.

Kiessling, W., and Baron-Szabo, R., 2004, Extinction and recovery patterns of scleractinian corals at the Cretaceous-Tertiary boundary: Palaeogeography, Palaeoclimatology, Palaeoecology, v. 214, p. 195–223, https://doi.org/10.1016/S0031-0182(04)00421-3.

Korbar, T., Montanari, A., Premec Fucek, V.P., Fucek, L., Coccioni, R., McDonald, I., Claeys, P., Schulz, T., and Koeberl, C., 2015, Potential Cretaceous-Paleogene boundary tsunami deposit in the intra-Tethyan Adriatic carbonate platform section of Hvar (Croatia): Geological Society of America Bulletin, v. 127, p. 1666–1680, https://doi.org/10.1130/B31084.1.

Korbar, T., McDonald, I., Premec Fucek, V.P., Fucek, L., and Posilovic, H., 2017, Post-impact event bed (tsunamite) at the Cretaceous-Paleogene boundary deposited on a distal carbonate platform interior: Terra Nova, v. 29, p. 135–143, https://doi.org/10.1111/ter.12257.

Laborel, J., and Laborel-Deguen, F., 1996, Biological indicators of Holocene sea-level and climatic variations on rocky coasts of tropical and subtropical regions: Quaternary International, v. 31, p. 53–60, https://doi.org/10.1016/1040-6182(95)00021-A.

Lein, R., 1982, Vorläufige Mitteilung über ein Vorkommen von flyschoider Gosau mit Komponenten paleozäner Riffkalke in den Mürztaler Alpen: Mitteilungen der Gesellschaft der Geologie- und Bergbaustudenten zu Wien, v. 28, p. 121–132.

Li, L., and Keller, G., 1998a, Diversification and extinction in Campanian-Maastrichtian planktic foraminifera of northwestern Tunisia: Eclogae Geologicae Helvetiae, v. 91, p. 75–102.

Li, L., and Keller, G., 1998b, Maastrichtian climate, productivity and faunal turnovers in planktic foraminifera in South Atlantic DSDP Sites 525A and 21: Marine Micropaleontology, v. 33, p. 55–86, https://doi.org/10.1016/S0377-8398(97)00027-3.

Li, L., and Keller, G., 1998c, Abrupt deep-sea warming at the end of the Cretaceous: Geology, v. 26, p. 995–998, https://doi.org/10.1130/0091-7613(1998)026<0995:ADSWAT>2.3.CO;2.

Li, L., Keller, G., Adatte, T., and Stinnesbeck, W., 2000, Late Cretaceous sea-level changes in Tunisia: A multi-disciplinary approach: Journal of the Geological Society, v. 157, p. 447–458, https://doi.org/10.1144/jgs.157.2.447.

Marriner, N., Kaniewski, D., Morhange, C., Flaux, C., Giaime, M., Vacchi, M., and Goff, J., 2017, Tsunamis in the geological record: Making waves with a cautionary tale from the Mediterranean: Science Advances, v. 3, p. e1700485, https://doi.org/10.1126/sciadv.1700485.

Massari, F., D'Alessandro, A., and Davaud, E., 2009, A coquinoid tsunamite from the Pliocene of Salento (SE Italy): Sedimentary Geology, v. 221, p. 7–18, https://doi.org/10.1016/j.sedgeo.2009.07.007.

Mateo, P., Keller, G., Adatte, T., and Spangenberg, J.E., 2016, Mass wasting during the Cretaceous-Paleogene transition in the North Atlantic: Relationship to the Chicxulub impact?: Palaeogeography, Palaeoclimatology, Palaeoecology, v. 441, p. 96–115, https://doi.org/10.1016/j.palaeo.2015.01.019.

Mateo, P., Keller, G., Punekar, J., and Spangenberg, E., 2017, Early to late Maastrichtian environmental changes in the Indian Ocean compared with Tethys and South Atlantic: Palaeogeography, Palaeoclimatology, Palaeoecology, v. 478, p. 121–138, https://doi.org/10.1016/j.palaeo.2017.01.027.

May, S.M., Vött, A., Brückner, H., Grapmayer, R., Handl, M., and Wennrich, V., 2012, The Lefkada barrier and beachrock system (NW Greece)—Controls on coastal evolution and the significance of extreme wave events: Geomorphology, v. 139–140, p. 330–347, https://doi.org/10.1016/j.geomorph.2011.10.038.

Moissette, P., Dulai, A., Escarguel, G., Kázmer, M., Müller, P., and Saint Martin, J.-P., 2007, Mosaic of environments recorded by bryozoan faunas from the middle Miocene of Hungary: Palaeogeography, Palaeoclimatology, Palaeoecology, v. 252, p. 530–556, https://doi.org/10.1016/j.palaeo.2007.05.010.

Molina, E., Alegret, L., Arenillas, I., Arz, J.A., Gallala, N., Hardenbol, J., von Salis, K., Steurbaut, E., Vandenberghe, N., and Zaghbib-Turki, D., 2006, The global boundary stratotype section and point for the base of the Danian Stage (Paleocene, Paleogene, "Tertiary," Cenozoic) at El Kef, Tunisia: Original definition and revision: Episodes, v. 29, p. 263–273.

Morton, R.A., Gelfenbaum, G., and Jaffe, B.E., 2007, Physical criteria for distinguishing sand tsunami and storm deposits using modern examples: Sedimentary Geology, v. 200, p. 184–207, https://doi.org/10.1016/j.sedgeo.2007.01.003.

Moura, D., Albardeiro, L., Veiga-Pires, C., Boski, T., and Tigano, E., 2006, Morphological features and processes in the central Algarve rocky coast (south Portugal): Geomorphology, v. 81, p. 345–360, https://doi.org/10.1016/j.geomorph.2006.04.014.

Moussavian, E., 1984, Die Gosau- und Alttertiärgerölle der Angerbergschichten (Höheres Oligozän, Unterinntal, Nördliche Kalkalpen): Facies, v. 10, p. 1–85, https://doi.org/10.1007/BF02536688.

Nebelsick, J.H., Rasser, M.W., and Bassi, D., 2005, Facies dynamics in Eocene to Oligocene circumalpine carbonates: Facies, v. 51, p. 197–217, https://doi.org/10.1007/s10347-005-0069-2.

Olsson, R.K., Hemleben, C., Berggren, W.A., and Huber, B.T., 1999, Atlas of Paleocene Planktonic Foraminifera: Washington, D.C., Smithsonian Institution Press, Smithsonian Contributions to Paleobiology 85, 252 p., https://doi.org/10.5479/si.00810266.85.1.

Ostermann, M., Sanders, D., Prager, C., and Kramers, J., 2007, Aragonite and calcite cementation in 'boulder-controlled' meteoric environments on the Fern Pass rockslide (Austria): Implications for radiometric age-dating of catastrophic mass movements: Facies, v. 53, p. 189–208, https://doi.org/10.1007/s10347-006-0098-5.

Perrin, C., 2002, Tertiary: The emergence of modern reef ecosystems, *in* Kiessling, W., Flügel, E., and Golonka, J., eds., Phanerozoic Reef Patterns: Society of Sedimentary Geology (SEPM) Special Publication 72, p. 587–621, https://doi.org/10.2110/pec.02.72.0587.

Piller, W.E., Egger, H., Erhart, C.W., Gross, M., Harzhauser, M., Hubmann, B., van Husen, D., Krenmayr, H.-G., Krystyn, L., Lein, R., Lukeneder, A., Mandl, G.W., Rögl, F., Roetzel, R., Rupp, C., Schnabel, W., Schönlaub, H.P., Summesberger, H., Wagreich, M., and Wessely, G., 2004, Die stratigraphische Tabelle von Österreich 2004 (sedimentäre Schichtfolgen): Wolkersdorf, Austria, Gerin Print, 1 p.

Platt, J.P., 1986, Dynamics of orogenic wedges and the uplift of high-pressure metamorphic rocks: Geological Society of America Bulletin, v. 97, p. 1037–1053, https://doi.org/10.1130/0016-7606(1986)97<1037:DOOWAT>2.0.CO;2.

Plaziat, J.-C., and Perrin, C., 1992, Multikilometer-sized reefs built by foraminifera (*Solenomeris*) from the early Eocene of the Pyrenean domain (S. France, N. Spain): Palaeoecologic relations with coral reefs: Palaeogeography, Palaeoclimatology, Palaeoecology, v. 96, p. 195–231, https://doi.org/10.1016/0031-0182(92)90103-C.

Plöchinger, B., 1967, Erläuterungen zur Geologischen Karte des Hohe-Wand-Gebietes (Niederösterreich): Vienna, Geologische Bundesanstalt, 148 p.

Punekar, J., Mateo, P., and Keller, G., 2014, Effects of Deccan volcanism on the paleoenvironment and planktic foraminifera: A global survey, *in* Keller, G., and Kerr, A., eds., Volcanism, Impacts and Mass Extinctions: Causes and Effects: Geological Society of America Special Paper 505, https://doi.org/10.1130/2014.2505(04), p. 91–116.

Punekar, J., Keller, G., Khozyem, H., Adatte, T., Font, E., and Spangenberg, J.E., 2016, A multi-proxy approach to decode the end-Cretaceous mass extinction: Palaeogeography, Palaeoclimatology, Palaeoecology, v. 441, p. 116–136, https://doi.org/10.1016/j.palaeo.2015.08.025.

Rasser, M.W., 1994, Facies and palaeoecology of rhodoliths and acervulinid macroids in the Eocene of the Krappfeld (Austria): Beiträge zur Paläontologie, v. 19, p. 191–217.

Rasser, M.W., 2000, Coralline red algal limestones of the late Eocene Alpine Foreland Basin in Upper Austria: Component analysis, facies and palecology: Facies, v. 42, p. 59–92, https://doi.org/10.1007/BF02562567.

Reuter, M., Piller, W.E., and Erhart, C., 2012, A middle Miocene carbonate platform under sili-volcaniclastic sedimentation stress (Leitha Limestone, Styrian Basin, Austria): Depositional environments, sedimentary evolution and palaeoecology: Palaeogeography, Palaeoclimatology, Palaeoecology, v. 350–352, p. 189–211, https://doi.org/10.1016/j.palaeo.2012.06.032.

Sanders, D., 1998, Tectonically controlled Late Cretaceous terrestrial to neritic deposition, Gosau Group, Northern Calcareous Alps (Tyrol, Austria): Facies, v. 39, p. 139–177, https://doi.org/10.1007/BF02537015.

Sanders, D., and Baron-Szabo, R., 1997, Coral-rudist bioconstructions in the Upper Cretaceous Haidach section (Northern Calcareous Alps, Austria): Facies, v. 36, p. 69–89, https://doi.org/10.1007/BF02536878.

Sanders, D., and Höfling, R., 2000, Carbonate deposition in mixed siliciclastic-carbonate environments on top of an orogenic wedge (Late Cretaceous, Northern Calcareous Alps, Austria): Sedimentary Geology, v. 137, p. 127–146, https://doi.org/10.1016/S0037-0738(00)00084-1.

Sanders, D., and Pons, J.M., 1999, Rudist formations in mixed siliciclastic-carbonate depositional environments, Upper Cretaceous, Austria: Stratigraphy, sedimentology, and models of development: Palaeogeography, Palaeoclimatology, Palaeoecology, v. 148, p. 249–284, https://doi.org/10.1016/S0031-0182(98)00186-2.

Sanders, D., Kollmann, H., and Wagreich, M., 1997, Sequence development and biotic assemblages on an active continental margin: The Turonian-Campanian of the Northern Calcareous Alps: Bulletin de la Société Géologique de France, v. 168, p. 351–372.

Schlagintweit, F., Studeny, M., and Sanders, D., 2016, *Clypeorbis*? *ultima* from the uppermost Maastrichtian of Austria: The youngest representative of the Clypeorbinae Sigal, 1952 (calcareous benthic foraminifera)?: Cretaceous Research, v. 66, p. 163–170, https://doi.org/10.1016/j.cretres.2016.06.006.

Schlagintweit, F., Sanders, D., and Studeny, M., 2018, The nepionic stage of *Solenomeris* Douvillé, 1924 (Acervulinidae, Foraminiferida): New observations from the uppermost Maastrichtian–early Danian of Austria (Kambühel Formation, Northern Calcareous Alps): Facies, v. 64, p. 27, https://doi.org/10.1007/s10347-018-0540-5.

Schoene, B., Samperton, K.M., Eddy, M.P., Keller, G., Adatte, T., Bowring, S.A., Khadri, S.F.R., and Gertsch, B., 2015, U-Pb geochronology of the Deccan Traps and relation to the end-Cretaceous mass extinction: Science, v. 347, p. 182–184, https://doi.org/10.1126/science.aaa0118.

Sedgwick, P.E., and Davis, R.A., 2003, Stratigraphy of washover deposits in Florida: Implications for recognition in the stratigraphic record: Marine Geology, v. 200, p. 31–48, https://doi.org/10.1016/S0025-3227(03)00163-4.

Sinnesael, M., De Vleeschouwer, D., Coccioni, R., Caeys, P., Frontalini, F., Jovane, L., Savian, J.F., and Montanari, A., 2016, High-resolution multiproxy cyclostratigraphic analysis of environmental and climatic events across the Cretaceous-Paleogene boundary in the classic pelagic succession of Gubbio (Italy), *in* Menichetti, M., Coccioni, R., and Montanari, A., eds., The Stratigraphic Record of Gubbio: Integrated Stratigraphy of the Late Cretaceous–Paleogene Umbria-Marche Pelagic Basin: Geological Society of America Special Paper 524, p. 115–137, https://doi.org/10.1130/2016.2524(09).

Sirel, E., 1998, Foraminiferal Description and Biostratigraphy of the Paleocene–Lower Eocene Shallow-Water Limestones and Discussion on the Cretaceous-Tertiary Boundary in Turkey: Ankara, Turkey, General Directorate of the Mineral Research and Exploration Monograph 2, 117 p.

Sirel, E., 2015, Reference sections and key localities of the Paleogene Stage and discussion on C-T, P-E and E-O boundaries by the very shallow-shallow water foraminifera in Turkey: Ankara University Yayinlari, v. 461, p. 1–171.

Sogot, C.E., Harper, E.M., and Taylor, P.D., 2013, Biogeographical and ecological patterns in bryozoans across the Cretaceous-Paleogene boundary: Implications for the phytoplankton collapse hypothesis: Geology, v. 41, p. 631–634, https://doi.org/10.1130/G34020.1.

Spencer, T., and Viles, H., 2002, Bioconstruction, bioerosion and disturbance on tropical coasts: Coral reefs and rocky limestone shores: Geomorphology, v. 48, p. 23–50, https://doi.org/10.1016/S0169-555X(02)00174-5.

Steuber, T., Mitchell, S.F., Buhl, D., Gunter, G., and Kasper, H.U., 2002, Catastrophic extinction of Caribbean rudist bivalves at the Cretaceous-Tertiary boundary: Geology, v. 30, p. 999–1002, https://doi.org/10.1130/0091-7613(2002)030<0999:CEOCRB>2.0.CO;2.

Stinnesbeck, W., Keller, G., De La Cruz, J., De León, C., MacLeod, N., and Whittacker, J.E., 1997, The Cretaceous-Tertiary boundary in Guatemala: Limestone breccia deposits from the South Peten Basin: Geologische Rundschau, v. 86, p. 686–709, https://doi.org/10.1007/s005310050171.

Stüben, D., Kramar, U., Berner, Z.A., Meudt, M., Keller, G., Abramovich, S., Adatte, T., Hambach, U., and Stinnesbeck, W., 2003, Late Maastrichtian paleoclimatic and paleoceanographic changes inferred from Sr/Ca ratio and stable isotopes: Palaeogeography, Palaeoclimatology, Palaeoecology, v. 199, p. 107–127, https://doi.org/10.1016/S0031-0182(03)00499-1.

Stüben, D., Harting, M., Kramar, U., Stinnesbeck, W., Keller, G., and Adatte, T., 2005, High resolution geochemical record in Mexico during the Cretaceous-Tertiary transition: Geochimica et Cosmochimica Acta, v. 69, p. 2559–2579, https://doi.org/10.1016/j.gca.2004.11.003.

Tantawy, A.A., Keller, G., Adatte, T., Stinnesbeck, W., Kassab, A., and Schulte, P., 2001, Maastrichtian to Paleocene (Dakhla Formation) depositional environment of the Western Desert in Egypt: Sedimentology, mineralogy and integrated micro- and macrofossil biostratigraphies: Cretaceous Research, v. 22, p. 795–827, https://doi.org/10.1006/cres.2001.0291.

Tantawy, A.A., Keller, G., and Pardo, A., 2009, Late Maastrichtian volcanism in the Indian Ocean: Effects on calcareous nannofossils and planktic foraminifera: Palaeogeography, Palaeoclimatology, Palaeogeography, v. 284, p. 63–87, https://doi.org/10.1016/j.palaeo.2009.08.025.

Thibault, N., and Husson, D., 2016, Climatic fluctuations and sea-surface water circulation patterns at the end of the Cretaceous Era: Calcareous nannofossil evidence: Palaeogeography, Palaeoclimatology, Palaeogeography, v. 441, p. 152–164, https://doi.org/10.1016/j.palaeo.2015.07.049.

Thibault, N., Galbrun, B., Gardin, S., Minoletti, F., and Le Callonec, L., 2016, The end-Cretaceous in the southwestern Tethys (Elles, Tunisia): Orbital calibration of paleoenvironmental events before the mass extinction: International Journal of Earth Sciences, v. 105, p. 771–795, https://doi.org/10.1007/s00531-015-1192-0.

Tobin, K.J., and Walker, K.R., 1996, Ordovician low- to intermediate-Mg calcite marine cements from Sweden: Marine alteration and implications for oxygen isotopes in Ordovician seawater: Sedimentology, v. 43, p. 719–735, https://doi.org/10.1111/j.1365-3091.1996.tb02022.x.

Tollmann, A., 1976, Analyse des klassischen nordalpinen Mesozoikums: Vienna, Austria, Franz Deuticke, 580 p.

Tragelehn, H., 1996, Maastricht und Paläozän am Südrand der Nördlichen Kalkalpen (Niederösterreich, Steiermark) [Ph.D. thesis]: Erlangen, Germany, University of Erlangen-Nürnberg, 216 p.

Trudgill, S.T., 1976, The marine erosion of limestone on Aldabra Atoll, Indian Ocean: Zeitschrift für Geomorphologie, Supplement Issues, v. 26, p. 164–200.

Tucker, M.E., and Wright, V.P., 1990, Carbonate Sedimentology: Oxford, UK, Blackwell Scientific, 482 p., https://doi.org/10.1002/9781444314175.

Twidale, C.R., Bourne, J.A., and Vidal Romani, J.R., 2005, Beach etching and shore platforms: Geomorphology, v. 67, p. 47–61, https://doi.org/10.1016/j.geomorph.2003.11.008.

Van Hinte, J.E., 1963, Zur Stratigraphie und Mikropaläontologie der Oberkreide und des Eozäns des Krappfeldes (Kärnten): Jahrbuch der Geologischen Bundesanstalt: Sonderband, v. 8, p. 1–147.

Vecsei, A., and Moussavian, E., 1997, Paleocene reefs on the Maiella platform margin, Italy: An example of the effects of the Cretaceous/Tertiary boundary events on reefs and carbonate platforms: Facies, v. 36, p. 123–139, https://doi.org/10.1007/BF02536880.

Vecsei, A., and Sanders, D., 1999, Facies analysis and sequence stratigraphy of a Miocene warm-temperate carbonate ramp, Montagna della Maiella, Italy: Sedimentary Geology, v. 123, p. 103–127, https://doi.org/10.1016/S0037-0738(98)00079-7.

Vecsei, A., Sanders, D., Bernoulli, D., Eberli, G.P., and Pignatti, J.S., 1998, Cretaceous to Miocene sequence stratigraphy and evolution of the Maiella carbonate platform margin, Italy, *in* Masse, J.-P., Jacquin, T., De Graciansky, P., and Vail, P.R., eds., Mesozoic and Cenozoic Sequence Stratigraphy of European Basins: Society of Sedimentary Geology (SEPM) Special Publication 60, p. 53–74, https://doi.org/10.2110/pec.98.02.0053.

Vellekoop, J., Smit, J., van de Schootbrugge, B., Weijers, J.W.H., Galeotti, S., Sinninghe Damsté, J.S., and Brinkhuis, J., 2015, Palynological evidence for prolonged cooling along the Tunisian continental shelf following the K-Pg boundary impact: Palaeogeography, Palaeoclimatology, Palaeoecology, v. 426, p. 216–228, https://doi.org/10.1016/j.palaeo.2015.03.021.

Vousdoukas, M.I., Velegrakis, A.F., and Plomaritis, T.A., 2007, Beachrock occurrence, characteristics, formation mechanisms and impacts: Earth-Science Reviews, v. 85, p. 23–46, https://doi.org/10.1016/j.earscirev.2007.07.002.

Wagreich, M., 2001, A 400-km-long piggyback basin (Upper Aptian–Lower Cenomanian) in the eastern Alps: Terra Nova, v. 13, p. 401–406, https://doi.org/10.1046/j.1365-3121.2001.00362.x.

Wagreich, M., and Faupl, P., 1994, Palaeogeography and geodynamic evolution of the Gosau Group of the Northern Calcareous Alps (Late Cretaceous, eastern Alps, Austria): Palaeogeography, Palaeoclimatology, Palaeoecology, v. 110, p. 235–254, https://doi.org/10.1016/0031-0182(94)90086-8.

Wang, P., and Horwitz, M.H., 2007, Erosional and depositional characteristics of regional overwash deposits caused by multiple hurricanes: Sedimentology, v. 54, p. 545–564, https://doi.org/10.1111/j.1365-3091.2006.00848.x.

Zuffa, G.G., 1985, Optical analyses of arenites: Influence of methodology on compositional results, *in* Zuffa, G.G., ed., Provenance of Arenites: North Atlantic Treaty Organization (NATO) Advanced Scientific Institution Series D: Dordrecht, Netherlands, Reidel Publishing Company, p. 165–189, https://doi.org/10.1007/978-94-017-2809-6_8.

Manuscript Accepted by the Society 9 September 2019